Natural and artificial radioactivity in surface waters of the Ebro river basin (Northeast Spain)

Ll. Pujol*, J.A. Sanchez-Cabeza

Departament de Física, Universitat Autònoma de Barcelona, ES-08193 Bellaterra, Barcelona, Spain

Abstract

A radiological characterisation of surface waters of the Ebro river basin was carried out during November 1994. For this purpose, 75 water samples were collected from points distributed throughout the Ebro river basin. Analysis included gross alpha and gross beta activities, relevant natural radionuclides (^{40}K, ^{226}Ra, ^{234,238}U -uranium total-) and several artificial radionuclides (^{3}H, ^{90}Sr and radiocaesium). Mean gross alpha and gross beta activities in surface waters of the river's main course were 0.095 ± 0.004 Bq l^{-1} and 0.213 ± 0.012 Bq l^{-1}, respectively. Mean activities of ^{40}K, ^{226}Ra and uranium (total) were 0.132 ± 0.009 Bq l^{-1}, 0.0282 ± 0.0008 Bq l^{-1} and 0.053 ± 0.006 Bq l^{-1}, respectively. Regarding artificial radionuclides, the mean ^{90}Sr activity was 6.6 ± 0.3 mBq l^{-1}, ^{3}H was detected in 8% of the samples, and radiocaesium was not detected in any sample. It is estimated that almost 100% of gross alpha and 97% of gross beta activities of surface waters in the Ebro river came from natural sources. Furthermore, results showed that the geological setting, large cities, agricultural areas and dams strongly influence the occurrence of natural radionuclides. Contamination from nuclear power plants located along the river was not detected. Finally, we estimated that the annual dose equivalent due to the hypothetical ingestion of Ebro river waters was 7.59 μSv y^{-1}, which represented only 0.3% of the average annual effective dose attributable to natural background radiation in the area.

* Corresponding author. Present address: Aplicaciones Isotópicas (CETA-CEDEX), 28014 Madrid, Spain.

1. Introduction

Radioactivity present in surface continental waters is mainly due to the presence of radioactive elements in the earth's crust (NORM, Naturally Occurring Radioactive Material). Recently, other artificial radionuclides have appeared due to such human activities as nuclear power plants, nuclear weapons testing and manufacture and use of radioactive sources. In addition, human activities (mining, milling and processing of uranium ores and mineral sands, manufacture of fertilisers, burning of fossils fuels, metal refining, etc.) have raised NORM concentrations in the environment. This is referred to as TERM (Technologically Enhanced Radioactive Material) or TENORM (Technologically Enhanced NORM) (Gesell & Prichard, 1975; Baxter, 1996; Egidi; 1997; Bradley & Roberts, 1998).

Radioactive material can reach surface continental waters by different pathways from each of the processes or activities that produce TERM. River water can be contaminated by surface runoff of rainwater transporting leached radionuclides from cities, mine waste, soil weathering, agricultural areas, and so on (Fetter, 1993; O'Brien & Cooper, 1998).

In order to determine the sources of TERM in the surface waters of the Ebro river, their overall contribution and relative importance, they have been classified into four groups:

- *Agricultural areas*. Agricultural fertiliser products contain various trace elements such as uranium and thorium decay series members and ^{40}K (NCRP, 1987). The use of fertilisers in agricultural areas can increase the concentration of these natural radionuclides in soils. For example, the potassium content of soils of arable lands is strongly influenced by the use of fertilisers (Eisenbud &

Gesell, 1997). Therefore, an appreciable fraction of radionuclides in continental waters results from erosion and run-off (Kathren, 1998).

- *Dams*. Suspended particulate matter and sediments carried by river waters can accumulate at the bottom of dams and become a source of radionuclides.
- *Extractive industries*. The extraction and processing of earth materials, or their industrial products or by-products, may increase the incorporation of radionuclides into the hydrosphere through surface and/or ground waters. Some relevant types of extractive and processing activities are (UNSCEAR, 1993; O'Brien & Cooper, 1998): i) coal-fired power plants (CPP) (Alvarez & Garzón, 1989), ii) phosphate fertiliser industries (Martínez-Aguirre & García-León, 1994) and iii) mining, milling and processing of uranium, mineral sands and coal (NCRP, 1993).
- *Large cities*. In river basins supporting considerable volumes of human activity, trace metals can be exported from urban or industrial areas via rainwater and runoff, and discharged into the aquatic ecosystem (Estèbe et al., 1998). Also, radioactive materials are found in a wide variety of commercial consumer products (NCRP, 1987): radioluminescent dials and markers, door bell pushes, electronic devices, smoke detectors, lantern mantles, ceramics, building materials and so on. For example, it has been demonstrated that the metal-refining industry can produce an increase in radioactivity (Lubenau & Yusko, 1995; Baxter et al., 1996).

In this work, we aimed to characterise a not well-known environment for which radiological information is scarce. This environment seems to be influenced by the presence of different radioactivity sources: NORM (basically the geological setting),

artificial radioactivity (nuclear power plants) and TERM (agricultural areas, dams, extractive industries and large cities). The radiological characterisation was carried out by sampling water from 75 locations distributed throughout the Ebro river basin. Gross alpha and gross beta activities in river waters were determined (WHO, 1993). As natural waters contain a number of both alpha and beta emitters in varying concentrations, it was considered useful to analyse some specific natural (^{40}K, ^{226}Ra and uranium -total-) and artificial (^{3}H, ^{90}Sr and radiocaesium) radionuclides in order to assess the relative importance of radioactivity sources in the river waters. Although ^{232}Th is abundant in rocks, its contribution to water's radioactivity is negligible because of its high insolubility (Scott, 1982; Eisenbud & Gesell, 1997).

2. Experimental section

2.1. Study area

The Ebro river basin is located in Northeast Spain. It is the largest Spanish fluvial system discharging into the Mediterranean Sea, with an approximate area of 85,000 km^2 and a river course 928 km long. The Ebro river basin covers several geological terrains: the sedimentary and metamorphic Palaeozoic terrains of the Iberian and Pyrenees mountains, the igneous terrains of these two areas and of the Priorat Massif, the sedimentary Mesozoic terrains of the Iberian Chain and the sedimentary Tertiary terrains of the Pre-Pyrenees and the Ebro Valley. The lower part of the Ebro river flows across the Neogene Mora Depression, bends through the Catalan Chain and the Baix Ebro Valley, and flows across the delta plain deposits (Marcuello, 1986; Guillén & Palanques, 1992) (Fig. 1).

The Ebro river monthly water discharge is quite irregular. Left-side tributaries provide a greater contribution to the discharge than those on the right-side (Fig. 1) because rainfall for left-side tributaries is more than 500 mm year^{-1} higher than for right-side tributaries. On

the other hand, water flow on the lower course of the Ebro river is highly regulated by dams, in particular, the Mequinenza dam (Fig. 2, H6[†]), which is located upstream from the Ascó nuclear power plant (Fig. 2, I6).

Some important mineral and rock deposits are located in the Ebro river basin (Ríos, 1983; CSCIM, 1996) (Fig. 1). Mineral sands, also called heavy minerals, originate from eroded inland rocks, and traces of them are subsequently transported towards surface waters (UNSCEAR, 1993).

Along the Ebro river course, large cities, agricultural areas, and non-nuclear enterprises such as chemical and phosphate industries, and coal-fired power plants are present. In particular, there are five lignite coal-fired power plants: Escucha (Fig. 2, G7), 175 MW (established in 1970); Teruel 1, 2 and 3 (Fig. 2, G7), 350 MW each (established in 1979) and Escatrón (Fig. 2, G6), 62.5 MW (established in 1990).

Nuclear Power Plants (NPP) are also present in i) Santa María de Garoña (Fig. 2, C3), with a 460 MW boiling water reactor (BWR), entered into operation in 1971, and ii) Ascó (Fig. 2, I6), on the lower section of the river, includes two pressurised water reactor (PWR) units, Ascó I (established in 1983) and Ascó II (1985), both of 930 MW.

2.2. Sampling

During November 1994, 75 water samples were collected along the Ebro river basin (Fig. 3). Sampling points were selected in the vicinity of NPPs, and upstream and downstream of large tributaries, sizeable cities and important industrial, mining and chemical areas (Table 1).

Surface water samples (250 ml) were collected to determine gross alpha, gross beta, radium, uranium (total) and tritium activity, using liquid scintillation counting (LSC), 100

[†] In order to help readers, the maps have been gridded with a letter and a number. Both letter and number are indicated in brackets.

ml to determine potassium concentration using atomic absorption spectrometry (AAS), and 20 ml to determine uranium concentration using fluorimetry. Large volume water samples were collected at 5 selected locations, next to the NPPs, to determine radiocaesium (100 l) and ^{90}Sr (30 l).

Special attention was given to sample collection and preservation (APHA-AWWA-WEF, 1998). Samples were collected in polyethylene bottles, which had been carefully washed in the laboratory before the sampling campaign. Water was collected at a certain distance from the riverbed and sufficiently far from the border, natural or artificial obstacles, and avoiding stagnant or turbid water zones. Before the sample was collected, containers were rinsed three times with flowing river water. Finally, samples were transported to the laboratory for analysis.

2.3. Sample preparation

Because surface raw water might carry large amounts of suspended solids that are removed during water treatment processes and would severely affect the measurement, filtering before analysis was carried out.

Use of sample acidification depends on the objective of the study. When considering radiological surveys, the particulate and colloidal fractions should not be considered as they are removed during water treatment procedures. Acidification after sample filtration would bring most metals associated with colloids into solution. Furthermore, the presence of acids strongly enhances quenching in liquid scintillation counting, which should be avoided when using this technique. Therefore, sample acidification was not performed.

In order to avoid possible ionic exchanges between suspended and dissolved matter during storage, samples were transferred to the laboratory for analysis within a short time

after collection. On the other hand, selected samples were prepared and measured several times. Results showed that the activity was constant over a long period of time, confirming the validity of the sampling and preparation techniques.

2.4. Analysis

Gross alpha, gross beta, radium, uranium (total), tritium, and ^{90}Sr counts were carried out using the liquid scintillation system Quantulus 1220. This detector system is specially designed for low-level counting of environmental samples. It has a pulse shape analysis (PSA) circuit which permits pulses produced by alpha and beta radiation to be discriminated by comparing the area of the pulse tail after 50 ns from the start with its total area. Pulse shape discrimination is achieved using a software adjustable parameter (PSA parameter) (Kaihola, 1990). Quenching is quantified with the SQP(E) parameter, which is used to determine the counting efficiency for each sample through calibration graphs. Samples, backgrounds and standards were simultaneously prepared and measured for all analyses when liquid scintillation was used.

It must be emphasised that a large number of commercial scintillation cocktails were available for water counting. However, only a few can hold a large amount of water and are biodegradable. Several studies were carried out in our laboratory (Pujol, 1996) and we finally decided to use OptiPhase Hisafe 3 for routine operation. This cocktail is based on the solvent called diisopropylnaphtalene, accepts about 50% of water in the counting mixture, and allows good pulse shape separation in alpha-beta counting. Furthermore, time stability of the mixture of the water solution and the scintillation cocktail was studied and we observed that this cocktail did not permeate through plastic vials for a long time (almost 12 months).

2.4.1. Gross alpha and gross beta

Gross alpha and gross beta activities were determined from one single measurement of the same sample. The counting parameters of the liquid scintillation system Quantulus 1220 were optimised for the best possible separation of the alpha and beta spectra. For normal quenching (that is, SQP(E) from 785 to 795, the range of values observed in water samples), the minimum interference occurred when using a pulse shape discrimination level of 117. For our counting conditions, the combination of OptiPhase Hisafe 3 in Zinsser low diffusion vials yielded a total interference of 1.69 ± 0.31 %. The simultaneous determination of gross alpha and gross beta activities in natural water samples was carried out as follows: each water sample (100 ml) was filtered, concentrated by evaporation (1:10), and 8 ml of the sample was mixed with 12 ml of the scintillation cocktail OptiPhase Hisafe 3 in Zinsser low diffusion vials (volume = 20 ml). Finally, samples were counted using a PSA parameter of 117 for 360 minutes. The detection limits attained were 0.012 Bq l^{-1} and 0.14 Bq l^{-1} for gross alpha and gross beta activities, respectively (Sanchez-Cabeza & Pujol, 1995; Pujol & Sanchez-Cabeza, 1997).

2.4.2. ^{226}Ra and uranium (total)

^{226}Ra and uranium (total) activities were determined simultaneously without radiochemical separation using liquid scintillation counting. Secular equilibrium of ^{226}Ra and its daughters is required, which is attained by storing the vial for 1 month after sample preparation. Radium activity was determined through ^{214}Po using an efficiency calibration curve, and uranium (total) activity was obtained from radium subtraction of the alpha spectrum. This method does not provide spectral information on uranium isotopes and, therefore, it is suitable for rough radiological surveys. The simultaneous determination of radium and uranium activities was carried out as follows: water samples (100 ml) were

filtered and concentrated by simple evaporation (1:10). Then, 8 ml of the sample was mixed with 12 ml of the scintillation cocktail OptiPhase Hisafe 3 in Zinsser low diffusion vials. Samples were stored for one month before counting. Samples were counted using a pulse shape parameter of 117. For a counting time of 360 minutes, the detection limits attained were 0.014 Bq l^{-1} and 0.033 Bq l^{-1} for radium and uranium determination, respectively (Sanchez-Cabeza & Pujol, 1998).

2.4.3. Tritium

Tritium activity was determined by mixing the water sample with an appropriate aqueous-accepting scintillation cocktail, without electrolytic enrichment. Therefore, minimal sample pre-treatment was required and sample preparation was rapid. The method for tritium determination was as follows: water samples were filtered, 8 ml of the filtrate was mixed with 12 ml of the scintillation cocktail OptiPhase Hisafe 3 (Wallac) in polyethylene vials (Wallac). Samples were stored in the liquid scintillation spectrometer for one day so that the chemiluminescence spectrum decreased. Samples were counted using a pulse shape parameter of 117. For a counting time of 360 minutes, the detection limit was 2.6 Bq l^{-1} (Pujol & Sanchez-Cabeza, 1999a). Although in the tritium spectrum there is some interference from natural or artificial beta emitters (such as ^{40}K, radium and uranium beta daughters, ^{90}Sr and ^{137}Cs) these are insignificant because tritium activities (ranging from < 2.6 Bq l^{-1} to 6.7 ± 0.9 Bq l^{-1}) are higher than gross beta activities (ranging from < 0.12 Bq l^{-1} to 0.30 ± 0.04 Bq l^{-1}).

2.4.4. ^{90}Sr

To determine ^{90}Sr activity, stable strontium was added as a yield tracer and carrier. Strontium was concentrated as an insoluble nitrate and purified from interfering

radionuclides. Colour quenching was avoided by removing the chromate ion through the precipitation of strontium as a nitrate. Then, the sample was dissolved in HCl and transferred into 20 ml polyethylene liquid scintillation vials (Wallac). After three weeks, ^{90}Sr was determined through its ^{90}Y daughter by Cerenkov counting using Quantulus 1220. In Cerenkov counting, little or no interference arises from the ^{90}Sr present because the mean ^{90}Sr beta energy (0.1957 MeV) approaches the threshold energy level for the production of Cerenkov radiation from electrons in aqueous solution (Harvey et al., 1989). For a 30 l sample and 360 minutes counting time, the detection limit achieved was 0.2 mBq l^{-1} (Pujol, 1996).

2.4.5. Radiocaesium

Caesium was concentrated by scavenging with ammonium molybdophosphate (AMP). Once the supernate was discarded, the AMP slurry was dried and placed in a geometry suitable for gamma counting. Previous work showed that the scavenging procedure is quantitative (Molero et al., 1993). The sample was measured for a minimum of 3×10^5 s using an HPGe detector surrounded by a 10 cm copper-cadmium-lead shield and linked to an 8K MCA with spectrum stabiliser. Spectra were analysed by means of a modified version of the SAMPO80 code (Koskelo et al., 1981). The detection limit attained was less than 1 mBq l^{-1} for a sample volume of 100 l.

2.4.6. Uranium mass concentration

As most uranium activities determined by the simple liquid scintillation counting method described were below the detection limit, a fluorimetric method was used to determine uranium mass concentrations (C_U) and, consequently, uranium activity (A_U)

through the equation

A_U (mBq l^{-1}) = C_U (μg l^{-1}) / 0.0804 (1)

In water, ^{238}U and ^{234}U can be found out of equilibrium due to geochemical processes. As a decay product, ^{234}U resides in the immediate vicinity of the parents, ^{238}U, ^{234}Th, and ^{234m}Pa. The energy released from the decay is thought to weaken the crystal structure in the immediate vicinity of the ^{234}U, thus increasing its mobility relative to ^{238}U. Therefore, if we assume that in surface natural waters $A_{U\text{-}234}$ = 1.25 $A_{U\text{-}238}$ approximately (Osmond & Ivanovich, 1992), then

$A_{U\text{-}234,238}$ (mBq l^{-1}) = 2.25 C_U (μg l^{-1}) / 0.0804 (2)

Uranium fluorescence was induced in a Scintrex UA-3 uranium analyser. One ml of the sample was mixed with 4 ml of Millipore water, the mixture was placed in the measurement cell and adjusted to zero. Thereafter, in order to enhance the uranium fluorescence, 1 ml of Fluran was added and the measurement was carried out. Results were compared with a uranyl nitrate standard to determine the uranium concentration (de Pablo et al., 1992). These analyses were carried out at the *Departament d'Enginyeria Química, Universitat Politècnica de Catalunya*.

2.4.7. Potassium mass concentration

Potassium mass concentration (C_K) was determined through atomic absorption spectrometry using a Perkin-Elmer 2100 system (APHA-AWWA-WEF, 1998). ^{40}K occurs to an extent of 0.0118% in natural potassium, thereby imparting a specific activity of 31.561 Bq g^{-1}. Because of its relative abundance and its energetic beta emission (E_{max} = 1.31 MeV), its contribution in the gross beta activity of the water is easily predominant in normal conditions.

The ^{40}K activity (A_{K-40}) was determined using the following relationship (Eisenbud & Gesell, 1997):

$$A_{K-40} \ (Bq\ l^{-1}) = 31.561\ Bq\ g^{-1}\ C_K\ (ppm) / 1000 \quad (3)$$

These analyses were carried out at the *Servei d'Anàlisi Química,Universitat Autònoma de Barcelona*.

2.4.8. Quality control

As low-level measurements require strict quality control assurance, blanks and reproducibility tests were periodically carried out. Also, the laboratory participates regularly in national and international intercomparison exercises. The results (Molero, 1992; Pujol, 1996) guaranteed the quality of our data, on which the accuracy of the interpretation depends.

2.5. Statistics

All statistical analyses were carried out with SPSS 7.5. First, distributions were explored for the presence of outliers, which were discarded from any further analysis. Then, normality was checked using the Kolmogorov-Smirnov test. As all resulting distributions were normal, the mean and standard error of the mean were determined. When comparing mean values, distributions with similar variances were compared using the Student t-test; otherwise, the Mann-Whitney test was used.

3. Results and discussion

The main objective of this work was to provide background information for future radiological studies in the Ebro basin, trying to relate basic radiological parameters with potential sources. It must be remarked that the information provided by gross activities is

sometimes difficult to interpret, since in order to fully identify the sources, it would be necessary to provide isotopic information. Therefore, the discussion derived from the results is, in some cases, based on assumptions and hypothesis carried out in an as yet poorly known environment.

3.1. Natural radioactivity

Results of gross alpha, gross beta, radium and uranium activity, and uranium (total) and potassium mass concentration are shown in Table 2. The statistical analysis of these results is included in Table 3.

3.1.1. Main course

Gross alpha activity averaged 0.095 ± 0.004 Bq l^{-1} and ranged from 0.07 to 0.15 Bq l^{-1} (excluding outliers). Gross alpha activity was below 0.11 ± 0.01 Bq l^{-1} from the river source to near the Mequinenza dam (Fig. 2, H6). A slight enhancement of gross alpha activity is observed in EB94ME65 and EB94MQ67 (see Table 2 and Figures 3 and 4). This can be explained by i) the presence of a coal-fired power plant next to the main course of the river (Fig. 2, G6), ii) the resuspension of the particulate matter accumulated at the bottom of the Mequinenza dam, and/or iii) the presence of lignite coal ores (Fig. 1, H6). Downstream, higher levels were observed again (Fig. 4). This slight enhancement in gross alpha levels in surface river waters can be explained by i) the leaching of radioactive material from granite rocks of the Priorat Massif (P) (Fig. 1, I6) after the Mequinenza dam and/or, ii) the impact from the chemical factory involved in phosphate production (Fig. 2, I6).

Gross beta activity averaged 0.213 ± 0.012 Bq l^{-1} and ranged from < 0.13 to 0.30 Bq l^{-1}. Gross beta activities increased downstream from urban centres such as Miranda (Fig. 2, C3) (from < 0.13 to 0.16 ± 0.04 Bq l^{-1}), Logroño (Fig. 2, D4) (from < 0.13 to 0.17

± 0.04 Bq l^{-1}) and Zaragoza (Fig. 2, G5) (from < 0.14 to 0.18 ± 0.04 Bq l^{-1}) (Fig. 5). This observation is consistent with the fact that downstream of urban or industrial areas there is an enhancement of trace metal concentrations (Estèbe, 1998). Gross beta activity increased from Zaragoza (Fig. 2, G5) to the Mequinenza dam (Fig. 2, H6) to a maximum of 0.30 ± 0.04 Bq l^{-1}. This can be explained by the increase in the potassium contents of waters from Zaragoza to the Mequinenza dam (Fig. 8) caused by the intensive use of fertilisers in this agricultural area (Fig. 2). The discharge of the Segre tributary (Fig. 5, H6) into the Ebro river caused a decrease in gross beta activity because of dilution with the Segre river waters, which showed lower activities than the Mequinenza dam.

^{226}Ra activity averaged 28.2 ± 0.8 mBq l^{-1} and ranged from 19 to 36 mBq l^{-1} (excluding outliers). Activity was homogeneous in all Ebro river waters (Fig. 6). These activities were similar to radium content of surface waters reported by other authors, namely 4 to 19 mBq l^{-1} (Eisenbud & Gesell, 1997).

Uranium (total) activity was detected by liquid scintillation counting only in five samples, all from the lower section of the river. The detection limit of uranium (total) was only 0.033 Bq l^{-1} using the liquid scintillation counting technique. For this reason fluorimetry was used to determine uranium mass concentration, which averaged 1.3 ± 0.2 μg l^{-1} and ranged from 0.04 to 3.53 μg l^{-1}. A slight but continuous increase in the uranium concentration from the river source to the Mequinenza dam (Fig. 2, H6) was observed (see Figure 7). The possible sources of uranium include i) the leaching of uranium from the rocks and soils in the river basin, and ii) the wastes from the phosphate industry (Fig. 2, E4, F5, I6). A significant rise in the uranium concentration was observed downstream from Mequinenza (Fig. 7), in agreement with the increase in gross alpha activity observed in this section and explained above. Although the mean concentration of uranium (total) in sea water is 3.3 μg l^{-1} (Cochran, 1982), that is, very similar to that observed in the last section

of the Ebro river downstream of the Mequinenza dam (Fig. 2, I6-7), further studies need to be carried out to confirm the intrusion of marine waters.

Potassium mass concentration averaged 4.1 ± 0.3 mg l^{-1} and ranged from 0.5 to 7.4 mg l^{-1}. From the Ebro source to Zaragoza city (Fig. 2, G5) a slight increase was observed. In the proximity of the city, the potassium concentration increased significantly, which may be explained by runoff of fertilisers from agricultural activities in this area (Fig. 2). Highest concentrations were observed at the Mequinenza dam (7.4 (±1-2%) mg l^{-1}). Downstream from the dam, potassium levels decreased due to dilution with the Segre river waters, which showed a lower concentration (Fig. 8). These results are in agreement with the trends of gross beta activity.

3.1.2. Left-side tributaries

Gross alpha activity averaged 0.103 ± 0.005 Bq l^{-1} and ranged from 0.06 to 0.16 Bq l^{-1}. In the Segre river, a relative increase in gross alpha activity (from 0.12 ± 0.01 to 0.16 ± 0.01 Bq l^{-1}) was observed downstream from Lérida city (Fig. 2, I5). This increase can be attributed to waste from the fertiliser industry (Fig. 2, I5) and/or urban wastes from this city.

Gross beta activity averaged 0.200 ± 0.010 Bq l^{-1} and ranged from < 0.13 to 0.27 Bq l^{-1}. A relative increase in gross beta activity was observed downstream from large cities, such as Vitoria (Fig. 2, D3) in the Zadorra river (from < 0.13 to 0.18 ± 0.04 Bq l^{-1}), Pamplona (Fig. 2, E3) in the Arga river (from < 0.13 to 0.19 ± 0.04 Bq l^{-1}) and Lérida (Fig. 2, I5) in the Segre river (from < 0.14 to 0.20 ± 0.04 Bq l^{-1}). The relative increase near the cities of Pamplona and Lérida may be attributed to the presence of potassium salt mines (Fig. 1, E3), and to fertilisers from agricultural activities (Fig. 2, I5). In the case of Vitoria however, no plausible hypothesis can be formulated.

^{226}Ra activity was similar to the mean observed in the main course, as it averaged 29.0 ± 0.8 mBq l^{-1} and ranged from 22 to 37 mBq l^{-1}.

Uranium activity (by liquid scintillation counting), was only detected in the Arba river (Fig 2, F5) (31 ± 16 mBq l^{-1}) and in the Segre river downstream of Lérida city (39 ± 18 mBq l^{-1}). Uranium mass concentration was variable, ranging from 0.08 to 4.37 μg l^{-1} and averaging 1.4 ± 0.3 μg l^{-1}. In general, mass concentrations were low, but levels in the Arba (4.37 ± 0.09 μg l^{-1}) and Segre rivers (4.36 ± 0.02 μg l^{-1}) were higher. The rise of uranium concentrations in the Segre river may be due to the impact of the fertiliser industry (Fig. 2, I5) and/or of urban wastes from this city. In the case of the Arba river, further studies need to be carried out.

Potassium mass concentrations ranged from 0.6 to 9.1 mg l^{-1} and averaged 3.6 ± 0.5 mg l^{-1}. In general, levels were lower than in the main course, but higher levels were observable in the Zadorra river after Vitoria city (Fig. 2, D3) (from 2.5 mg l^{-1} to 9.1 mg l^{-1}) and in the Arga river after Pamplona city (Fig. 2, E3) (from 1.4 mg l^{-1} to 8.6 mg l^{-1}) (see Figure 8). These observations are consistent with gross beta activities. The increase near Pamplona city may be attributed to the presence of potassium salt mines (Fig. 1, E3). In the case of Vitoria, the source of potassium is not known.

3.1.3. Right-side tributaries

Gross alpha activity averaged 0.132 ± 0.007 Bq l^{-1} and ranged from 0.09 to 0.16 Bq l^{-1} (excluding outliers). In some cases, gross alpha activities were particularly high: 0.37 ± 0.02 Bq l^{-1} in the Alhama river (Fig. 2, E4-5), 0.47 ± 0.03 Bq l^{-1} in the Martín river (Fig. 2, G6-7) and 0.32 ± 0.02 Bq l^{-1} in the Guadalope river (Fig. 2, G8&H6-7). However, these activities did not cause a significant increase in the main course activity because their discharge was small. Gross beta activity averaged 0.24 ± 0.01 Bq l^{-1} and ranged from <

0.12 to 0.29 Bq l^{-1} (excluding outliers). Similarly, gross beta activity in the Martín river (Fig. 2, G6-7) was 0.40 ± 0.08 Bq l^{-1}, while in the Guadalope river (Fig. 2, G8&H6-7) it was 0.39 ± 0.06 Bq l^{-1}. Mining of coal and minerals can bring up appreciable amounts of uranium, thorium and the members of their radioactive series, which may enter surface waters. It is shown in Figure 1 that there is a considerable presence of mining in this area. In particular, there is considerable mining of lignite near the Martín and Guadalope rivers.

^{226}Ra activity averaged 29 ± 1 mBq $^{l-1}$, ranged from < 17 to 37 mBq l^{-1} (excluding outliers) and presented its highest levels in the basin. ^{226}Ra activity in the Alhama river (Fig. 2, E4-5) was 68 ± 11 mBq l^{-1} and, in the Martín river (Fig. 2, G6-7) it was 64 ± 12 mBq l^{-1}. These activities were statistically higher than those observed in the Ebro river basin.

Uranium mass concentration averaged 2.1 ± 0.2 μg l^{-1}, and ranged from 0.59 to 3.5 μg l^{-1} (excluding outliers). The highest uranium concentrations were observed in the Guadalope river (Fig. 2, G8&H6-7) (5.9 ± 0.2 μg l^{-1}) and in the Martín river (Fig. 2, G6-7) (3.5 ± 0.9 μg l^{-1}). Apart from the significant mining activity of this region, the impact of nearby coal-fired power plants cannot be discarded, as these are known to redistribute uranium traces in their vicinity (Fig. 2, G7). Further work is necessary to identify the sources of these relatively high uranium concentrations.

Potassium mass concentration averaged 5.1 ± 0.5 mg l^{-1} and ranged from 2.3 to 8.2 mg l^{-1} (excluding outliers). The Alhama (Fig. 2, E4-5), Martín (Fig. 2, G6-7) and Cidacos (Fig. 2, E4) rivers presented the highest potassium mass concentrations in the basin (see Fig. 8), namely 13.8 (±1-2%) mg l^{-1}, 11.5 (±1-2%) mg l^{-1} and 10.6 (±1-2%) mg l^{-1}, respectively. This may be explained by i) the lower dilution of these rivers as discharge is lower in this area, ii) the mining of ores and minerals in the area (Fig. 1) which may bring up potassium.

3.1.4. Discussion

Several works (Vallés et al, 1994; Pujol, 1996; Sanchez-Cabeza & Pujol, 1998) have shown that the main natural radionuclide contributions to gross activities in the Ebro river waters are uranium (total) and radium and its alpha daughters for gross alpha activity, and ^{40}K and ^{226}Ra beta daughters for gross beta activity.

3.1.4.1. Main course

Gross alpha activity variation in the Ebro river waters from its source to the Mequinenza dam was negligible. Upstream (close to the dam) and downstream higher levels were observed due to a significant increase of uranium concentrations in the water. ^{226}Ra activity was almost homogeneous throughout all Ebro river waters. Several reasons may explain this uranium enhancement: i) the presence of a coal-fired power plant next to the main course of the river (Fig. 2, G6), ii) the resuspension of the particulate matter accumulated at the bottom of Mequinenza dam, iii) the presence of lignite coal ores (Fig. 1, H6), iv) the leaching of radioactive material from granite rocks of the Priorat Massif (P) (Fig. 1, I6) after the Mequinenza dam, and v) the phosphate chemical plant (Fig. 2, I6).

Gross beta activity was only detectable, from the river source next to the Mequinenza dam, downstream of large cities, such as Miranda (Fig. 2, C3), Logroño (Fig. 2, D4) and Zaragoza (Fig. 2, G5). Downstream of Zaragoza city to the Mequinenza dam, gross beta activity increased. This is consistent with the high potassium concentration observed in the water, and may be due to runoff of fertilisers from agricultural activities in the area (Fig. 2). Downstream of the dam, potassium levels decreased due to dilution with the Segre river waters.

3.1.4.2. Left-side tributaries

Gross alpha activity was homogeneous for all tributaries. Only in two locations, downstream of Lérida city (Fig. 2, I5) and on Arba river (Fig. 2, F5), were observed higher levels of uranium. The significant increase of uranium in the Segre river may be due to fertiliser industry and/or urban wastes.

Gross beta activity is not detectable below 0.14 Bq l^{-1} in most sampling locations. There is a significant increase downstream of large cities such as Vitoria (Fig. 2, D3), Pamplona (Fig. 2, E3) and Lérida (Fig. 2, I5). This increase is consistent with the higher levels of potassium concentration. The sources of potassium appear to be i) the presence of potassium salt mines (Fig. 1, E3) in the case of Pamplona, and ii) agricultural activity (Fig 2) in the case of Lérida. No plausible interpretation can be offered for the increase observed near Vitoria.

3.1.4.2. Right-side tributaries

Mean gross alpha activity in the right-side tributaries is higher than in the main course and in the left tributaries, in agreement with the higher mean uranium concentration in this area. On the other hand, the Alhama (Fig. 2, E4-E5), Martín (Fig. 2, G6-7) and Guadalope rivers (Fig. 2, G8&H6-7) present gross alpha activities ranging from 0.32 to 0.47 Bq l^{-1}. In these locations ^{226}Ra presents the highest levels of the basin. The enhancement of gross alpha activity in these samples is mainly due to ^{226}Ra and its alpha daughters.

Mean gross beta activity in the right-side tributaries is higher than in the main course and left-side tributaries, in keeping with the higher mean potassium concentration in this area.

The source of uranium and potassium would seem to be the considerable presence of mining in the right-side tributary sub-basins. In particular, lignite mining is present on the Martín and Guadalope rivers (Fig. 1, G7) along with a number of coal-fired power plants (Fig. 2, G7).

3.2. Artificial radioactivity

3.2.1. Tritium

Tritium was only detected in rivers close to the Pyrenees Mountains (Fig.1, F2-L2), namely the Aragón (Fig. 2, E4&F3-G3) and Arga (Fig. 2, E3) rivers (Table 4). For this reason, a mean value was not provided in this work. As tritium was only detected far away from NPPs it seems reasonable to attribute the origin of this tritium both to i) fallout of spallation products, produced by the interaction in the atmosphere of stable nuclei with cosmic radiation and ii) fallout of atmospheric nuclear detonations. In the latter case tritium, which was mainly deposited in the early 60s, was incorporated into long residence time environments such as groundwater, lakes (Murphy, 1993) and/or glaciers.

It must be emphasised that during normal operation, the Ascó NPP (Fig. 2, I6) generates low-activity radioactive liquid waste, including tritium, which is released into the river in a controlled way. In previous papers, tritium releases were used to study the hydrodynamics of the Ebro river waters (Pujol & Sanchez-Cabeza, 1999b; Sanchez-Cabeza & Pujol, 1999). However, no tritium was detected in this sampling campaign.

3.2.2. ^{90}Sr

^{90}Sr activities were uniform, averaging 6.6 ± 0.3 mBq l^{-1} and ranging from 5.9 to 7.6 mBq l^{-1} (Table 5). Activities upstream and downstream of NPPs were statistically indistinguishable, as confirmed by the Student t-test for equality of means. Therefore, ^{90}Sr

in the Ebro river waters could be attributed solely to global fallout, and the impact of the plant had little, if any, significance. This has been confirmed by previous work (Sanchez-Cabeza et al., 1999).

^{90}Sr is highly soluble in fresh and ground waters (Coughtrey & Thorne, 1983). Therefore, its widespread presence in surface continental waters is due to leaching and runoff of global fallout radiostrontium with both surface and ground waters in the Ebro river basin (Sanchez-Cabeza et al., 1999).

3.2.3. Radiocaesium

Although the detection limit for radiocaesium was very low, that is, less than 1 mBq l^{-1}, it was not detected in the vicinity of any NPP during this sampling campaign. In previous work, authors detected the presence of ^{134}Cs and ^{137}Cs downstream of Ascó NNP (Fig. 2, I6), (2.3 ± 1.0 mBq l^{-1} and 2.4 ± 0.8 mBq l^{-1}, respectively, mean value for several samples from 1989 to 1993) most if not all of which, attributable to radiocaesium contamination from the plant (Sanchez-Cabeza et al., 1999).

3.2.4. Discussion

Sampling was designed in order to obtain a fair description of relevant artificial radionuclides in the Ebro river basin. For this reason, ^{3}H, ^{90}Sr and radiocaesium deserved special attention. Although in previous work higher levels of ^{3}H (Pujol and Sanchez-Cabeza, 1999b; Sanchez-Cabeza & Pujol, 1999) and radiocaesium were detected (Sanchez-Cabeza et al., 1999), in this study, radiocaesium was not detected and tritium levels were low or undetectable. On the other hand, ^{90}Sr levels were statistically unchanged upstream and downstream of NPPs. Therefore, we can conclude that the sources of the artificial radionuclides studied in this work are fallout of spallation products produced in

the atmosphere and fallout of atmospheric nuclear detonations, and that the contamination from NPPs is negligible.

The enhancement of tritium in rivers close to the Pyrenees Mountains must be pointed out. This could be used to study the residence time of water in environments such as groundwater or lakes in the Pyrenees.

3.3. Dose estimation

The simplest freshwater-human pathway is water consumption. Although river water is treated before consumption, a conservative assumption for dose estimation is that a member of the public would drink water with the same radioactivity contents as raw river water. As the Ebro river water collected at Xerta (Fig. 3, I7, EB94XE74) is used for human consumption after treatment, we used the concentration observed at that location to compute the dose received from the consumption of drinking water (Table 6). We used dose conversion factors published by the International Commission of Radiological Protection (ICRP) Publication 68 (1994), which are based on the recommendations of ICRP Publication 60 (1991). The dose calculation was based upon an adult drinking water intake of 2 litres per day for 1 year. The contribution of drinking water to the total exposure is very small and is largely due to naturally occurring radionuclides. We estimated that the annual dose equivalent due to the ingestion of the Ebro river waters was only 7.59 $\mu Sv\ y^{-1}$. This value is similar to that reported in another work (Sanchez-Cabeza et al., 1996), and by other authors (Vallés et al., 1994) and it represented only 0.3% of the average effective dose attributable to natural background radiation, that is, 2.4 mSv per year (UNSCEAR, 1993). Natural radionuclides represented 98.3% of this dose.

A more realistic estimation of dose assessment in the Ebro river should include other pathways such as irrigation, fish consumption, shoreline recreation and swimming

(Linsalata et al., 1986; Pujol & Sanchez-Cabeza, 1998). However, this did not come within the scope of the objectives of the present work.

3.4. Radioactivity in river waters of the world

The levels of gross alpha, gross beta and ^{40}K activities; radium and uranium activities; and tritium, ^{90}Sr and ^{137}Cs activities in a number of rivers around the world are shown in Tables 7, 8 and 9, respectively. Results observed in the main course of the Ebro river are not dissimilar to those observed in other European and world rivers.

4. Conclusions

The main objective of this work was to provide background information for future radiological studies in the Ebro basin, trying to relate basic radiological parameters with potential sources. It must be remarked that the information provided by gross activities is sometimes difficult to interpret since in order to fully identify the sources, it would be necessary to provide isotopic information. The main conclusions can be summarised as follows:

1. Most of the radioactivity present in the surface waters of the Ebro river was natural. We can assume that the gross alpha activity derived mainly from uranium and radium and its alpha daughters, and that the gross beta was mostly due to ^{40}K, ^{226}Ra beta daughters and ^{90}Sr. We estimated that the gross alpha activity was composed of ^{226}Ra and its alpha daughters (65%) and uranium (total) (35%), and the gross beta activity was composed of ^{40}K (54%), ^{226}Ra and its beta daughters (43%), and ^{90}Sr (3%) (Tables 3 and 5).
2. The enhancement of gross alpha activity in the main course of the Ebro river and left-side tributaries is mainly due to the increase in uranium concentration. In the right-side tributaries the enhancement is mainly due to ^{226}Ra and its daughters.

3. The possible sources of gross alpha activity in the main course of the Ebro river were i) the presence of a coal-fired power plant next to the main course of the river (Fig. 2, G6), ii) the resuspension of the particulate matter accumulated at the bottom of the Mequinenza dam, iii) the presence of lignite coal ores (Fig. 1, H6), iv) the leaching of radioactive material from granite rocks of the Priorat Massif (P) (Fig. 1, I6) after the Mequinenza dam and/or, v) the phosphate production plant (Fig. 2, I6). Large cities do not seem to be a source of gross alpha activity.
4. The possible sources of gross alpha activity in the right-side tributaries appeared to be lignite mining in the Martín and Guadalope river basins (Fig. 1, G7) and several coal-fired power plants (Fig. 2, G7) in this area.
5. The enhancement of gross beta activity in the main course of the Ebro river and in the left and right-side tributaries is mainly due to the increase in potassium concentration.
6. The possible sources of gross beta activity in the main course of the Ebro river and in the left-side tributaries are i) large cities, ii) the runoff of fertilisers from agricultural activities in this area (Fig. 2), iii) the resuspension of the particulate matter accumulated at the bottom of the Mequinenza dam, and iv) the presence of potassium salt mines.
7. The sources of gross beta activity in the right-side tributaries seem to be the considerable presence of mining activities in the area, because the extraction and processing of earth materials may increase the incorporation of radionuclides into surface water by run-off and/or leaching.
8. The sources of artificial radionuclides studied in this work (^{3}H, ^{90}Sr, radiocaesium) can be attributed to the fallout of spallation products produced in the atmosphere, and to the fallout from atmospheric nuclear detonations. The contribution from NPPs is negligible.
9. The annual dose equivalent due to ingestion of Ebro river water was estimated to be 7.59 $\mu Sv\ y^{-1}$, which represented only 0.3% of the average annual effective dose

attributable to natural background radiation. Natural radioactivity represented 98.3% of the total dose estimation.

Acknowledgements

The authors gratefully acknowledge help during sampling campaigns and the technical support of our colleagues in the Physics Department. This work was funded by the *Junta de Sanejament de la Generalitat de Catalunya.*

References

Alvarez, M.C., & Garzón, L.(1989). Assessment of radiological emissions from spanish coal power plants: radioactive releases and associated risks. *Health Physics, 57*, 765-769.

APHA-AWWA-WEF (1998). *Standard Methods for the Examination of Water and Wastewater*. Washington: American Public Health Association.

Bradley, D.A., & Roberts, C. (1998). Foreword. *Applied Radiation Isotopes*, *49*, 147-148.

Baxter, M.S. (1996). Technologically enhanced radioactivity: an overview. *Journal of Environmental Radioactivity*, *32*, 3-17.

Baxter, M.S., MacKenzie, A.B., East, B.W., & Scott, E.M. (1996). Natural decay series radionuclides in and around a large metal refinery. *Journal of Environmental Radioactivity*, *32*, 115-133.

Carreiro, M.C.V., & Sequeira, M.M.A. (1994). Radiactividade artificial nos rios Tejo e Guadiana: 1989-1993. In *5ºCongreso de la Sociedad Española de Protección Radiológica*, SEPR, Santiago, pp. 318-324 (in Portuguese).

Carreiro, M.C.V., Bettencourt, A.O., & Sequeira, M.M.A. (1991). Radioécologie du Tage, 1981-1989. *Radioprotection*, *26*, 649-663 (in French).

CBRMC (Comité de bassin Rhône Méditerranée Corse) (1992). *Synthèse des Connaisances sur la Radioécologie du Rhône*. Service d'Études et de Recherches sur les transferts dans l'Environment (SERE) de l'Institut de Protection et de Sûreté Nucléaire (IPSN), Centre de Cadarache, Saint Paul-lez-Durance, Cedex (in French).

Cochran, J.K. (1982). The oceanic chemistry of the U- and Th- series nuclides. In M. Ivanovich, & R.S. Harmon (Eds.), *Uranium Series Disequilibrium. Applications to Environmental Problems* (pp. 384-430). Oxford: Clarendon Press.

Coughtrey, P.J., & Thorne, M.C. (1983). *Radionuclide Distribution and Transport in Terrestrial and Aquatic Ecosystems*, (Vol. I). Rotterdam: A.A. Balkema.

CSCIM (Consejo Superior de Colegios de Ingenieros de Minas) (1996*). La Minería en España – Situación actual y posibilidades de desarrollo* (3 Vol.). Madrid: CSCIM (in Spanish).

CSN (Consejo de Seguridad Nuclear) (1993). Informe al Congreso de los Diputados y al Senado, CSN/IS/25/93, Madrid, pp. 342-352 (in Spanish).

de Pablo J., Duro, L., Giménez, J., Havel, J., Torrero, M.E., & Casas, I. (1992). Fluorometric determination of traces of uranium (VI) in brines and iron (III) oxides using separation on an actived silica gel column. *Analytica Chimica Acta*, *264*, 115-119.

Descamps, B., & Foulquier, L. (1988). Natural radioactivity in the principal constituents of French river ecosystems. *Radiation Protection Dosimetry*, *24*, 143-147.

Egidi, P. (1997). *Introduction to naturally occurring radioactive material*. 42nd Annual Meeting of the Health Physics Society, USA.

Eisenbud, M., & Gesell, T. (1997). *Environmental Radioactivity*. New York: Academic Press.

Estèbe, A., Mouchel, J.M., & Thévenot, D.R. (1998). Urban runoff impacts on particulate metal concentrations in river seine. *Water, Air and Soil Pollution*, *108*, 83-105.

Fetter, C.W. (1993). *Contaminant Hydrogeology*. New York: Macmillan Publishing Company.

Fukai R., Ballestra, S., Thein, M., & Guion, J. (1981). Input of transuranic elements through rivers into the Mediterranean sea. In *Impacts of Radionuclide Releases into the Marine Environment*. IAEA-SM-248/125, IAEA, Viena, pp. 3-14.

Gesell, T. F., & Prichard, H. M. (1975). The technologically enhanced natural radiation environment. *Health Physics*, *28*, 361-366.

Guillén, J., & Palanques, A. (1992). Sediment dynamics and hydrodynamics in the lower course of a river highly regulated by dams: the Ebro River. *Sedimentology*, *39*, 567-579.

Harvey, B.H., Ibbet, R.D., Lovett, M. B., & Williams K.J. (1989). Analytical procedures for the determination of strontium radionuclides in environmental materials. In *Aquatic Environment Protection: Analytical Methods 5*. Ministry of Agriculture Fisheries and Food, Directorate of Fisheries Research, Lowestoft.

Hesketh, G. E. (1982). Natural radioactivity in water. *Journal of the Society for Radiological Protection*, *2*, 11-14.

ICRP (1991). 1990 recommendations of the International Commision on Radiological Protection. ICRP Publication 60. *Annals of the ICRP*, *21* (1-3). Oxford: Pergamon Press.

ICRP (1994). Dose coefficients for intakes of radionuclides by workers. ICRP Publication 68. *Annals of the ICRP*, *24* (4). Oxford: Pergamon Press.

Kaihola, L. (1990). Ultra low background liquid scintillation spectrometry of alpha particles. In *International Seminar on Low-level Counting in Environmental Radioactivity Monitoring*, Estonian Academy of Sciencies, Tallinn.

Kathren, R.L. (1998). NORM sources and their origins. *Applied Radiation Isotopes*, *49*, 149-168.

Kobal, I., Vaupotic, J., Mitic, D., Kristan, J., Ancik, M., Jerancic, S., & Škofljanec, M. (1990). Natural radioactivity of fresh waters in Slovenia, Yugoslavia. *Environmental International*, *16*, 141-154.

Koskelo, M.J., Aarnio, P.A., & Routti, J.T. (1981). SAMPO80: Microcomputer program for gamma spectrum analysis with nuclide identification. *Comp. Phys. Comm.*, *24*, 11-35.

Linsalata, P., Hickman, D., & Cohen, N. (1986). Comparative pathway analysis of radiocesium in the Hudson river estuary: environmental measurements and regulatory dose assessment models. *Health Physics*, *51*, 295-312.

Lubenau, J.O., & Yusko, J.G. (1995). Radioactive materials in recycled metals. *Health Physics*, *68*, 440-451.

Marcuello, J.R. (1986). *El Ebro*. Zaragoza: Ediciones Oroel (in Spanish).

Martín Sánchez, A., Vera Tomé, F., & Díaz Bejarano, J., (1987). Natural isotopic separation of uranium in the Guadiana river. *Journal of Radioanalytical and Nuclear Chemistry, Letters*, *118*, 291-298.

Martínez-Aguirre, A., & García-León, M. (1991). Natural radioactivity enhacement by human activities in rivers of the southwest of Spain. *J. Radioanal. Nucl. Chem., Letters*, *155*, 97-106.

Martínez-Aguirre, A., & García-León, M. (1992). Uranium and radium isotopes in the Guadalquivir river, Southern Spain. *Radiation Protection Dosimetry*, *45*, 249-252.

Martínez-Aguirre, A., & García-León, M. (1994). The distribution of U, Th and 226Ra derived from the phosphate fertiliser industries on an estuarine system in southwest Spain. *J. Environ. Radioactivity*, *22*, 155-177.

Molero, J. (1992). *Comportamiento y Distribución de los Radionúclidos de Vida Larga en Ecosistemas Marinos. Estudio Relativo a Radiocesio y a los Transuránidos Plutonio y Americio en el Entorno Ambiental de la Costa Mediterránea Española*. PhD Thesis, Universidad Autònoma de Barcelona, Spain (in Spanish).

Molero, J., Morán, A., Sanchez-Cabeza, J.A., Blanco, M., Mitchell, P.I., & Vidal-Quadras, A. (1993). Efficiency of radiocaesium concentration from large volume natural water samples by scavenging with ammonium moliybdophosphate. *Radiochimica Acta*, *62*, 159-162.

Murphy, C.E. (1993). Tritium transport and cycling in the environment. *Health Physics*, *65*, 683-697.

NCRP (National Council on Radiation Protection and Measurement) (1987). *Radiation exposure of the U.S. population from consumer products and miscellaneous sources*. NCRP Report No. 95, Washington.

NCRP (1993). *Radiation Protection in the mineral extraction industry*. NCRP Report No. 118, Washington.

O'Brien, R.S., & Cooper, M.B. (1998). Technologically enhanced naturally occurring radioactive material (NORM): pathway analysis and radiological impact. *Applied Radiation Isotopes*, *49*, 227-239.

Osmand, J.K, & Ivanovich, M. (1992). Uranium-series mobilization and surface hydrology. In M. Ivanovich, & R.S. Harmon (Eds.), *Uranium-Series Disequilibrium: Applications to Earth, Marine and Environmental Sciences*, (pp. 259-289). Oxford: Clarendon Press.

Pujol, Ll. (1996). Radiactividad del agua superficial y los sedimentos en la cuenca del Ebro. Utilización del tritio como radiotrazador en el tramo catalán. PhD Thesis, Universitat Autònoma de Barcelona, Spain (in Spanish).

Pujol, Ll., & Sanchez-Cabeza, J.A. (1997). Role of quenching on alpha/beta separation in liquid scintillation counting for several high capacity cocktails. *Analyst*, *122*, 383-385.

Pujol, Ll., & Sanchez-Cabeza, J.A. (1998). Estimación de la dosis recibida vía hidrosfera en una población del tramo catalán del río Ebro. Radioprotección, Nº extraordinario, 463-465 (in Spanish).

Pujol, Ll., & Sanchez-Cabeza, J.A. (1999a). Optimisation of liquid scintillation counting conditions for rapid tritium determination in aqueous samples. *Journal of Radioanalytical and Nuclear Chemistry*, *242*, 391-398.

Pujol, Ll. & Sanchez-Cabeza, J.A. (1999b). Determination of longitudinal dispersion coefficient and velocity of the Ebro river waters (Northeast Spain) using tritium as a radiotracer. *Journal of Environmental Radioactivity*, *45*, 39-57.

Ríos, J.M. (1983). *Geología de España* (Vol. 2). Madrid: Instituto Geológico y Minero de España (in Spanish).

Rodríguez, M.J. (1993). *Determinación por Espectrometría Alfa de las Actividades de Uranio Presentes en Aguas del Río Júcar*. Master Thesis. Centro Mixto C.S.I.C - Universidad de Valencia (in Spanish).

Sanchez-Cabeza, J.A., & Pujol, Ll. (1995). A rapid method for the simultaneous determination of gross alpha and beta activities in water samples using a low background liquid scintillation counter. *Health Physics*, ***68***, 674-682.

Sanchez-Cabeza, J.A., & Pujol, Ll. (1996). Gross alpha and beta activities in natural waters using low-background liquid scintillation: study of the Ebro river (Spain). In G.T. Cook, D.D. Harkness, A.B. MacKenzie, B.F. Miller, & E.M. Scott (Eds.), *Liquid Scintillation Spectrometry 1994* (pp.307-316). Tucson: Radiocarbon.

Sanchez-Cabeza, J.A., & Pujol, Ll. (1998). Simultaneous determination of radium and uranium activities in water samples using liquid scintillation counting. *Analyst*, *123*, 399-403.

Sanchez-Cabeza, J.A., & Pujol, Ll. (1999). Study on the hydrodynamics of the Ebro river lower course using tritium as a radiotracer. *Water Research*, *33*, 2345-2356.

Sanchez-Cabeza, J.A., Pujol, Ll., Merino, J., Bruach, J.M., & Molero, J. (1999). Artificial radionuclides in waters of the lower section of the river Ebro (Northeast Spain). *Water, Air and Soil Pollution*, *133*, 1-19.

Scott, M.R. (1982). The Chemistry of U and Th series nuclides in rivers. In M. Ivanovich, & R.S. Harmon (Eds.), *Uranium Series Disequilibrium: Applications to Environmental Problems* (pp. 181-201). Oxford: Clarendon Press.

Szabò, A. S. (1993). *Radioecology and Environmental Protection*. New York: Ellis Horwood.

UNSCEAR (1993). *Ionizing Radiation: Sources and Effects of ionizing radiation*. New York: United Nations.

Vallés, I., Ortega, X., & Serrano I. (1994). Contribución de la radiactividad de las aguas potables en la zona de Cataluña a la dosis por ingestión. In *Actas del 5º Congreso Nacional de la Sociedad Española de Protección Radiológica*, SEPR, Santiago, pp. 361-368 (in Spanish).

Vera Tomé, F., Martín Sánchez, A., & Díaz Bejanaro, J. (1988). Activity ratios of natural uranium in surface waters. *J. Radioanal. Nucl. Chem., Letters*, *126*, 419-427.

WHO (World Health Organisation) (1993). *Guidelines for drinking-water quality*, *Recommendations, Volume 1* (pp. 114-121). Geneva: OMS.

Table 1
Water samples collected along the Ebro basin during November 1994. Sample codes are EB94XXYY, where EB corresponds to the **EB**ro river, **94** is the sampling year, XX is the sampling location and YY is the sampling location number (Figure 3) .

Sample Code	Location	Sampling date	River	Latitude (N)	Longitude (E)	Sample code	Location	Sampling date	River	Latitude (N)	Longitude (E)
EB94AR01	Artesa de Segre	10/11/94	Segre	41º 55'00"	1º 04'45"	EB94FI39	Fitero	15/11/94	Alhama	42º 03'30"	- 1º 51'45"
EB94CA02	Embalse de Camarasa	10/11/94	Noguera Pallar.	41º 56'15"	0º 51'45"	EB94CA40	Castejón	15/11/94	Ebro	42º 10'45"	- 1º 41'45"
EB94BA03	Balaguer	10/11/94	Segre	41º 47'15"	0º 48'30"	EB94MI41	Milagro	15/11/94	Aragón	42º 14'30"	- 1º 45'15"
EB94CO04	Corbins	11/11/94	Noguera Ribag.	41º 41'45"	0º 42'00"	EB94BU42	Buñuel	16/11/94	Ebro	41º 58'15"	- 1º 26'00"
EB94LL05	Lérida	11/11/94	Segre	41º 39'15"	0º 39'45"	EB94TA43	Tauste	16/11/94	Arba	41º 54'45"	- 1º 16'45"
EB94AI06	Aitona	11/11/94	Segre	41º 29'00"	0º 27'45"	EB94RE44	Remolinos	16/11/94	Ebro	41º 51'00"	- 1º 14'00"
EB94FR07	Fraga	11/11/94	Cinca	41º 31'45"	0º 20'45"	EB94CA45	Cabañas	16/11/94	Ebro	41º 47'30"	- 1º 08'00"
EB94BA08	Ballobar	11/11/94	Alcanadre	41º 37'15"	0º 11'45"	EB94AL46	Alagón	16/11/94	Jalón	41º 45'30"	- 1º 06'30"
EB94AL09	Alcolea de Cinca	11/11/94	Cinca	41º 43'30"	0º 08'00"	EB94MO47	Monzalbarba	16/11/94	Ebro	41º 42'30"	- 0º 57'15"
EB94SA10	Sabiñánigo	11/11/94	Gállego	42º 31'30"	- 0º 22'00"	EB94ZA48	Zaragoza	16/11/94	Gállego	41º 40'15"	- 0º 50'30"
EB94AS11	Áscara	11/11/94	Aragón	42º 33'30"	- 0º 39'30"	EB94MA49	S. Mateo de Gállego	16/11/94	Gállego	41º 49'15"	- 0º 47'15"
EB94SA12	Sangüesa	12/11/94	Aragón	42º 34'30"	- 1º 17'15"	EB94ZU50	Zuera	16/11/94	Gállego	41º 52'30"	- 0º 46'45"
EB94HU13	Huarte	12/11/94	Arga	42º 50'00"	- 1º 35'00"	EB94PI51	Pina	18/11/94	Ebro	41º 29'30"	- 0º 32'15"
EB94OR14	Ororbia	12/11/94	Arga	42º 48'45"	- 1º 44'45"	EB94BU52	El Burgo de Ebro	18/11/94	Ebro	41º 35'45"	- 0º 46'45"
EB94PU15	Puente de la Reina	12/11/94	Arga	42º 40'30"	- 1º 49'15"	EB94MO53	Morata de Jiloca	18/11/94	Jiloca	41º 15'15"	- 1º 35'00"
EB94AR16	Arínzazo	12/11/94	Ega	42º 38'00"	- 1º 59'30"	EB94TE54	Terrer	18/11/94	Jalón	41º 19'30"	- 1º 42'30"
EB94IG17	Iguzquiza	12/11/94	Ega	42º 39'30"	- 2º 05'45"	EB94ES55	Escatrón	19/11/94	Ebro	41º 17'30"	- 0º 18'00"
EB94DU18	Durana	12/11/94	Zadorra	42º 53'30"	- 2º 38'30"	EB94ES56	Escatrón	19/11/94	Martín	41º 17'15"	- 0º 18'45"
EB94VI19	Villodas	12/11/94	Zadorra	42º 50'15"	- 2º 47'00"	EB94SA57	Sástago	19/11/94	Ebro	41º 19'15"	- 0º 20'30"
EB94FO20	Fontibre	13/11/94	Ebro	43º 01'15"	- 4º 12'00"	EB94GE58	Gelsa	19/11/94	Ebro	41º 24'00"	- 0º 28'30"
EB94BA21	Bárcena de Ebro	13/11/94	Ebro	42º 51'15"	- 4º 02'00"	EB94AR59	Ariño	19/11/94	Martín	41º 04'00"	- 0º 33'30"
EB94BA22	Bárcena de Ebro	13/11/94	Polla	42º 51'15"	- 4º 02'15"	EB94OL60	Oliete	19/11/94	Martín	40º 59'15"	- 0º 41'30"
EB94ES23	Escalada	13/11/94	Ebro	42º 48'30"	- 3º 46'30"	EB94MO61	Montalbán	19/11/94	Martín	40º 50'00"	- 0º 47'45"
EB94TE24	Terminón	13/11/94	Oca	42º 43'30"	- 3º 26'30"	EB94AL62	Aliaga	20/11/94	Guadalope	40º 40'30"	- 0º 42'00"
EB94TR25	Traspaderne	13/11/94	Nela	42º 48'00"	- 3º 23'30"	EB94CA63	Calanda	20/11/94	Guadalope	40º 55'45"	- 0º 12'15"
EB94FR26	Frías	14/11/94	Ebro	42º 46'15"	- 3º 17'15"	EB94CS64	Caspe	20/11/94	Guadalope	41º 12'45"	0º 00'45"
EB94MA27	San Martín de Don	14/11/94	Ebro	42º 46'00"	- 3º 10'30"	EB94ME65	Embalse Mequinenza	20/11/94	Ebro	41º 15'45"	- 0º 03'45"
EB94SU28	Suzano	14/11/94	Ebro	42º 42'00"	- 2º 58'30"	EB94MZ66	Mequinenza	21/11/94	Segre	41º 22'30"	0º 18'15"
EB94LE29	Leiba	14/11/94	Tirón	42º 30'30"	- 3º 03'00"	EB94MQ67	Embalse Mequinenza	21/11/94	Ebro	41º 22'00"	0º 15'30"
EB94HA30	Haro	14/11/94	Ebro	42º 35'30"	- 2º 50'30"	EB94MN68	Embalse Mequinenza	21/11/94	Ebro	41º 21'45"	0º 17'00"
EB94VI31	San Vicente	14/11/94	Ebro	42º 33'45"	- 2º 45'45"	EB94MA69	Fayón	21/11/94	Matarraña	41º 13'50"	0º 20'30"
EB94TO32	Torremontalbo	14/11/94	Najerilla	42º 30'00"	- 2º 41'00"	EB94RR70	Ribarroja	21/11/94	Ebro	41º 14'40"	0º 25'45"
EB94PU33	La Puebla de la Barca	14/11/94	Ebro	42º 29'30"	- 2º 34'30"	EB94FL71	Flix	21/11/94	Ebro	41º 13'45"	0º 33'15"
EB94LO34	Logroño	15/11/94	Iregua	42º 27'15"	- 2º 25'15"	EB94AS72	Ascó	21/11/94	Ebro	41º 11'05"	0º 34'20"
EB94AL35	Alcanadre	15/11/94	Ebro	42º 25'00"	- 2º 07'15"	EB94MV73	Miravet	21/11/94	Ebro	41º 02'00"	0º 36'35"
EB94SA36	Sartaguda	15/11/94	Ebro	42º 22'30"	- 2º 03'15"	EB94XE74	Xerta	21/11/94	Ebro	40º 55'25"	0º 29'30"
EB94AN37	Andosilla	15/11/94	Ega	42º 22'30"	- 1º 56'45"	EB94AM75	Amposta	21/11/94	Ebro	40º 42'45"	0º 35'10"
EB94AU38	Autol	15/11/94	Cidacos	42º 13'00"	- 2º 00'00"						

Table 2
Gross alpha, gross beta, radium and uranium activity and uranium and potassium concentration in water samples along the Ebro river basin

River	Sample code	Gross alpha (Bq l^{-1})	Gross beta (Bq l^{-1})	Radium (mBq l^{-1})	Uranium (mBq l^{-1})	Uranium (µg l^{-1})	Uranium† (mBq l^{-1})	Potassium (ppm)	Potassium‡ (Bq l^{-1})
Ebro	EB94FO20	0.11 ± 0.01	< 0.14	32 ± 5	< 36	0.14 ± 0.01	3.9 ± 0.3	1.7	0.05
	EB94BA21	0.09 ± 0.01	< 0.13	35 ± 6	< 35	0.19 ± 0.02	5.3 ± 0.6	2.8	0.09
	EB94ES23	0.09 ± 0.01	< 0.13	32 ± 3	< 33	0.45 ± 0.03	12.6 ± 0.8	3.7	0.12
	EB94FR26	0.08 ± 0.01	< 0.13	28 ± 5	< 32	0.04 ± 0.01	1.1 ± 0.3	0.5	0.02
	EB94MA27	0.09 ± 0.01	< 0.13	31 ± 5	< 34	0.50 ± 0.01	14.0 ± 0.3	2.1	0.07
	EB94SU28	0.09 ± 0.01	0.16 ± 0.04	25 ± 5	< 29	0.44 ± 0.05	12 ± 1	4.3	0.14
	EB94HA30	0.07 ± 0.01	0.21 ± 0.04	29 ± 5	< 31	0.43 ± 0.04	12 ± 1	4.0	0.13
	EB94VI31	0.09 ± 0.01	< 0.13	32 ± 5	< 34	0.66 ± 0.03	18.5 ± 0.8	3.7	0.12
	EB94PU33	0.08 ± 0.01	< 0.13	26 ± 5	< 36	0.50 ± 0.01	14.0 ± 0.3	2.9	0.09
	EB94AL35	0.08 ± 0.01	0.17 ± 0.04	26 ± 5	< 30	0.40 ± 0.01	11.2 ± 0.3	3.8	0.12
	EB94SA36	0.11 ± 0.01	0.14 ± 0.04	34 ± 6	< 36	0.71 ± 0.03	19.9 ± 0.8	3.0	0.09
	EB94CA40	0.08 ± 0.01	< 0.13	32 ± 6	< 33	0.53 ± 0.03	14.8 ± 0.8	4.0	0.13
	EB94BU42	0.08 ± 0.01	< 0.13	28 ± 5	< 32	0.52 ± 0.01	14.6 ± 0.3	4.0	0.13
	EB94RE44	0.08 ± 0.01	< 0.12	21 ± 4	< 27	0.96 ± 0.04	27 ± 1	2.8	0.09
	EB94CA45	0.10 ± 0.01	0.19 ± 0.04	25 ± 5	< 31	0.92 ± 0.01	25.7 ± 0.3	2.7	0.09
	EB94MO47	0.09 ± 0.01	< 0.14	19 ± 4	< 29	0.99 ± 0.02	27.7 ± 0.6	5.0	0.16
	EB94BU52	0.09 ± 0.01	0.18 ± 0.04	20 ± 4	< 29	1.18 ± 0.01	33.0 ± 0.3	5.3	0.17
	EB94PI51	0.10 ± 0.01	< 0.13	28 ± 5	< 30	1.22 ± 0.06	34 ± 2	5.5	0.18
	EB94GE58	0.10 ± 0.01	0.17 ± 0.04	32 ± 6	< 33	1.45 ± 0.02	40.6 ± 0.6	5.9	0.19
	EB94SA57	0.10 ± 0.01	0.24 ± 0.04	24 ± 5	< 31	0.39 ± 0.07	11 ± 2	5.3	0.17
	EB94ES55	0.09 ± 0.01	0.18 ± 0.04	26 ± 5	< 31	1.41 ± 0.03	39.5 ± 0.8	5.6	0.18
	EB94ME65	0.12 ± 0.01	0.21 ± 0.04	27 ± 5	< 32	1.32 ± 0.01	36.9 ± 0.3	5.5	0.17
	EB94MQ67	0.15 ± 0.01	0.30 ± 0.04	21 ± 5	51 ± 17	1.76 ± 0.07	49 ± 2	7.3	0.23
	EB94MN68	0.13 ± 0.01	0.30 ± 0.04	30 ± 5	< 34	1.93 ± 0.06	54 ± 2	7.4	0.23
	EB94RR70	0.19 ± 0.01*	0.28 ± 0.04	42 ± 6*	< 38	3.10 ± 0.09	87 ± 3	4.0	0.13
	EB94FL71	0.19 ± 0.01*	0.23 ± 0.04	26 ± 5	69 ± 18	3.20 ± 0.08	90 ± 2	4.4	0.14
	EB94AS72	0.20 ± 0.01*	0.24 ± 0.04	36 ± 6	40 ± 20	3.4 ± 0.4	95 ± 11	4.1	0.13
	EB94MV73	0.18 ± 0.01*	0.14 ± 0.04	27 ± 5	65 ± 18	3.5 ± 0.2	98 ± 6	4.1	0.13
	EB94XE74	0.17 ± 0.01*	0.27 ± 0.04	32 ± 5	< 35	3.53 ± 0.09	99 ± 3	4.1	0.13
	EB94AM75	0.18 ± 0.01*	0.22 ± 0.04	33 ± 6	42 ± 19	3.3 ± 0.1	92 ± 3	4.4	0.14
Nela	EB94TR25	0.09 ± 0.01	< 0.13	37 ± 6	< 36	0.08 ± 0.01	2.2 ± 0.3	1.5	0.05
Zadorra	EB94DU18	0.10 ± 0.01	< 0.13	27 ± 5	< 32	0.13 ± 0.01	3.6 ± 0.3	2.5	0.08
	EB94VI19	0.07 ± 0.01	0.18 ± 0.04	25 ± 5	< 29	0.13 ± 0.01	3.6 ± 0.3	9.1	0.29
Ega	EB94IG17	0.11 ± 0.01	< 0.14	32 ± 5	< 35	0.36 ± 0.01	10.1 ± 0.3	2.7	0.09
	EB94AR16	0.09 ± 0.01	< 0.13	33 ± 6	< 34	0.34 ± 0.01	9.5 ± 0.3	2.6	0.08
	EB94AN37	0.10 ± 0.01	< 0.14	33 ± 5	< 36	0.56 ± 0.01	15.7 ± 0.3	2.4	0.08
Aragón	EB94AS11	0.08 ± 0.01	< 0.14	28 ± 5	< 35	0.31 ± 0.03	8.7 ± 0.8	0.6	0.02

	EB94SA12	0.07 ± 0.01	< 0.14	29 ± 5	< 34	0.13 ± 0.03	3.6 ± 0.8	1.1	0.03
	EB94HU13	0.07 ± 0.01	< 0.13	29 ± 5	< 33	0.157 ± 0.002	4.39 ± 0.06	1.4	0.04
	EB94OR14	0.06 ± 0.01	0.19 ± 0.04	22 ± 5	< 31	0.11 ± 0.01	3.1 ± 0.3	8.6	0.27
	EB94PU15	0.11 ± 0.01	0.18 ± 0.04	25 ± 5	< 32	n.d.	n.d.	8.3	0.26
	EB94MI41	0.09 ± 0.01	< 0.13	28 ± 5	< 33	0.33 ± 0.01	9.2 ± 0.3	3.1	0.10
Arba	EB94TA43	0.12 ± 0.01	0.23 ± 0.04	22 ± 4	31 ± 16	4.37 ± 0.09	122 ± 3	6.0	0.19
Gállego	EB94SA10	0.08 ± 0.01	< 0.13	23 ± 5	< 31	0.21 ± 0.03	5.9 ± 0.8	3.7	0.12
	EB94ZU50	0.11 ± 0.01	< 0.13	26 ± 5	< 35	1.55 ± 0.02	38.3 ± 0.6	5.2	0.16
	EB94MA49	0.12 ± 0.01	0.18 ± 0.04	27 ± 5	< 36	1.5 ± 0.1	43 ± 3	5.1	0.16
	EB94ZA48	0.10 ± 0.01	0.22 ± 0.04	32 ± 6	< 34	0.84 ± 0.04	24 ± 1	6.8	0.21
Segre	EB94AR01	0.08 ± 0.01	< 0.14	34 ± 6	< 38	1.07 ± 0.02	29.9 ± 0.6	1.8	0.06
	EB94CA02	0.10 ± 0.01	< 0.14	33 ± 5	< 40	0.8 ± 0.1	22 ± 3	0.8	0.03
	EB94BA03	0.12 ± 0.01	< 0.14	35 ± 6	< 40	1.94 ± 0.02	54.3 ± 0.6	2.7	0.09
	EB94CO04	0.14 ± 0.01	0.17 ± 0.04	27 ± 5	< 33	3.9 ± 0.2	109 ± 6	3.9	0.12
	EB94LL05	0.12 ± 0.01	< 0.14	37 ± 6	< 39	2.9 ± 0.1	81 ± 3	1.6	0.05
	EB94AI06	0.16 ± 0.01	0.20 ± 0.04	27 ± 5	39 ± 18	4.36 ± 0.02	122.0 ± 0.6	4.2	0.13
	EB94FR07	0.13 ± 0.01	0.16 ± 0.04	32 ± 5	< 35	2.2 ± 0.2	62 ± 6	2.6	0.08
	EB94BA08	0.12 ± 0.01	0.18 ± 0.04	24 ± 5	< 30	3.36 ± 0.05	94 ± 1	5.0	0.16
	EB94AL09	0.10 ± 0.01	< 0.14	32 ± 5	< 37	0.85 ± 0.04	24 ± 1	1.4	0.04
	EB94MZ66	0.13 ± 0.01	0.27 ± 0.04	25 ± 5	< 32	3.58 ± 0.05	100 ± 1	3.3	0.10
Oca	EB94TE24	0.14 ± 0.01	0.19 ± 0.04	37 ± 6	< 36	2.2 ± 0.1	62 ± 3	5.9	0.19
Tirón	EB94LE29	0.15 ± 0.01	< 0.13	30 ± 5	< 34	1.76 ± 0.04	49 ± 1	3.2	0.10
Najerilla	EB94TO32	0.12 ± 0.01	< 0.14	30 ± 5	< 36	0.9 ± 0.1	25 ± 3	2.3	0.07
Iregua	EB94LO34	0.09 ± 0.01	< 0.12	29 ± 5	< 33	0.59 ± 0.07	17 ± 2	2.6	0.08
Cidacos	EB94AU38	0.12 ± 0.01	0.26 ± 0.04	< 17	< 29	2.10 ± 0.07	59 ± 2	10.6*	0.33*
Alhama	EB94FI39	0.37 ± 0.02*	< 0.28	68 ± 11*	< 77	2.11 ± 0.09	59 ± 3	13.8*	0.44*
Jalón	EB94MO53	0.16 ± 0.01	0.23 ± 0.04	22 ± 5	58 ± 17	2.58 ± 0.06	72 ± 2	5.2	0.16
	EB94TE54	0.15 ± 0.01	0.27 ± 0.04	28 ± 5	< 33	1.91 ± 0.03	53.5 ± 0.8	6.4	0.20
	EB94AL46	0.13 ± 0.01	0.22 ± 0.04	33 ± 5	< 36	2.5 ± 0.1	70 ± 3	6.3	0.20
Martín	EB94MO61	0.14 ± 0.01	0.25 ± 0.04	24 ± 5	< 32	2.11 ± 0.05	59 ± 1	6.0	0.19
	EB94OL60	0.16 ± 0.01	0.29 ± 0.04	34 ± 6	< 37	2.5 ± 0.2	70 ± 6	7.5	0.24
	EB94AR59	0.37 ± 0.03*	< 0.35	64 ± 12*	< 89	3.1 ± 0.1	87 ± 3	7.6	0.24
	EB94ES56	0.47 ± 0.03*	0.40 ± 0.08*	49 ± 10*	240 ± 38*	3.5 ± 0.9	98 ± 25	11.5*	0.36*
Guadalope	EB94AL62	0.09 ± 0.01	< 0.13	26 ± 5	< 32	1.12 ± 0.01	31.3 ± 0.3	2.4	0.08
	EB94CA63	0.11 ± 0.01	0.21 ± 0.04	29 ± 5	< 33	1.13 ± 0.08	32 ± 2	3.6	0.11
	EB94CS64	0.32 ± 0.02*	0.39 ± 0.06*	45 ± 8*	134 ± 31*	5.9 ± 0.2*	165 ± 6*	8.2	0.26
Matarraña	EB94MA69	0.16 ± 0.01	0.23 ± 0.04	26 ± 5	34 ± 17	2.9 ± 0.1	81 ± 3	4.0	0.13

Uncertainties correspond to ±1σ. Uncertainties of potassium range (1-2)%. for ± 1σ. (*) Outlier.

†$A_{U\text{-}234,238}$ (mBq l^{-1}) = 2.25 C_U (μg l^{-1}) / 0.0804; ‡$A_{K\text{-}40}$ (Bq l^{-1}) = 31.561 Bq g^{-1} C_K (ppm) / 1000

Table 3
Statistical analyses of gross alpha, gross beta, radium and uranium activity and uranium and potassium concentration in water along the Ebro river. The Ebro river values correspond only to the main course. Outliers were excluded from the analysis. The analysis technique is shown (LSC: Liquid Scintillation Counting; AAS: Atomic Absorption Spectrometry).

Area	Gross alpha ($Bq\ l^{-1}$) LSC	Gross beta ($Bq\ l^{-1}$) LSC	Radium ($mBq\ l^{-1}$) LSC	Uranium ($mBq\ l^{-1}$) LSC	Uranium ($\mu g\ l^{-1}$) Fluorimetry	Uranium† ($mBq\ l^{-1}$)	Potassium (ppm) AAS	Potassium‡ ($Bq\ l^{-1}$)
Basin								
Range	0.06 – 0.16	< 0.13 – 0.30	< 17 – 37	< 27 – 69	0.04 – 4.37	1 – 122	0.5 – 9.1	0.02 – 0.29
Median (N)	0.10 (64)	0.21 (38)	28 (68)	42 (9)	1.13 (72)	32 (72)	4 (71)	0.13 (71)
Mean	0.106 ± 0.003	0.241 ± 0.007	28.7 ± 0.5	48 ± 5	1.50 ± 0.15	42 ± 4	4.1 ± 0.2	0.131 ± 0.007
Ebro river								
Range	0.07 – 0.15	< 0.13 – 0.30	19 – 36	< 27 – 69	0.04 – 3.53	1 – 99	0.5 – 7.4	0.02 – 0.23
Median (N)	0.09 (24)	0.21 (18)	28 (29)	51 (5)	0.94 (30)	26.3 (30)	4.05 (30)	0.13 (30)
Mean	0.095 ± 0.004	0.213 ± 0.012	28.2 ± 0.8	53 ± 6	1.3 ± 0.2	36 ± 5	4.1 ± 0.3	0.132 ± 0.009
Left tributaries								
Range	0.06 – 0.16	< 0.13 – 0.27	22 – 37	< 29 – 39	0.08 – 4.37	2 – 122	0.6 – 9.1	0.02 – 0.29
Median (N)	0.10 (27)	0.18 (11)	28 (27)	35 (2)	0.82 (26)	22.9 (26)	2.7 (27)	0.09 (27)
Mean	0.103 ± 0.005	0.200 ± 0.010	29.0 ± 0.8	35 ± 4	1.4 ± 0.3	39 ± 8	3.6 ± 0.5	0.114 ± 0.015
Right tributaries								
Range	0.09 – 0.16	< 0.12 – 0.29	< 17 – 37	< 29 – 58	0.59 – 3.50	17 – 98	2.3 – 8.2	0.07 - 0.26
Median (N)	0.14 (13)	0.23 (9)	29 (12)	46 (2)	2.1 (16)	59 (16)	5.5 (14)	0.17 (14)
Mean	0.132 ± 0.007	0.24 ±0.01	29 ± 1	43 ± 12	2.1 ± 0.2	59 ± 6	5.1 ± 0.5	0.161 ± 0.018

Uncertainties correspond to ±1σ. Uncertainties of potassium ranged (1-2)%.

†$A_{U\text{-}234,238}$ ($mBq\ l^{-1}$) = 2.25 C_U ($\mu g\ l^{-1}$) / 0.0804; ‡$A_{K\text{-}40}$ ($Bq\ l^{-1}$) = 31.561 $Bq\ g^{-1}$ C_K (ppm) / 1000

Table 4
Tritium activities in water samples along the Ebro river basin

Sample	River	Concentration ($Bq\ l^{-1}$)
EB94SA12	Aragón	4.8 ± 0.9
EB94HU13	Arga	5.3 ± 0.9
EB94OR14	Arga	6.6 ± 0.9
EB94PU15	Arga	6.7 ± 0.9
EB94AR16	Ega	3.4 ± 0.8
EB94AL35	Ebro	3.3 ± 0.8

Uncertainties correspond to ±1σ.

Table 5
^{90}Sr activity in water samples along the Ebro river basin

Date	Sample code	Situation	Concentration (mBq l^{-1})
14/11/94	EB94FR26	Upstream Garoña	6.2 ± 0.9
14/11/94	EB94MA27	Downstream Garoña	5.9 ± 1.4
20/11/94	EB94MQ67	Middle location	6.8 ± 1.0
21/11/94	EB94RR70	Upstream Ascó	7.6 ± 1.2
21/11/94	EB94MV73	Downstream Ascó	6.7 ± 1.1
Range			*5.9 - 7.6*
Mean			*6.6 ± 0.3*

Uncertainties correspond to ±1σ.

Table 6
Dose estimation from drinking Ebro river water

Radionuclide	**Activity ($Bq\ m^{-3}$)**	**Dose conversion factor † ($Sv\ Bq^{-1}$)**	**Dose ($\mu Sv\ y^{-1}$)**
^{40}K	132	$6.2 \cdot 10^{-9}$	0.60
^{226}Ra ‡	28.2	$2.8 \cdot 10^{-7}$	5.76
$^{238}U + {}^{234}U$	32	$4.7 \cdot 10^{-8}$	1.10
Total natural			*7.46*
^{90}Sr		$2.8 \cdot 10^{-8}$	0.13
	6.6		
Total artificial			*0.13*
Total			***7.59***

†(ICRP, 1994). Dose factor for $^{238}U + {}^{234}U$ was averaged.
‡ Includes short-lived daughter products.

Table 7
Gross alpha, gross beta and potassium activity in water from a number of rivers around the world

River	Gross alpha ($Bq\ l^{-1}$)	Gross beta ($Bq\ l^{-1}$)	^{40}K ($Bq\ l^{-1}$)	Reference	Location, date
Ebro	0.02 - 0.12	0.07 - 0.30	0.05 - 0.18	CSN, 1993	Spain, 1992†
Tajo	0.01 - 0.12	0.05 - 0.19	0.03 - 0.30	CSN, 1993	Spain, 1992†
Guadiana	0.06	0.80	0.60	CSN, 1993	Balbuena (Spain), 1992
Duero	0.01	0.05	0.03	CSN, 1993	Soria (Spain), 1992
Sava		0.016 - 0.215		Kobal et al., 1990	Slovenia, 1975
Severn	0.11 - 0.33	0.41	0.10 - 0.15	Hesketh, 1982	United Kingdom, 1970
Danubio		0.11 - 0.40		Szabo, 1993	Hungary, 1962-1970
Ebro	**0.095 ± 0.004**	**0.213 ± 0.012**	**0.132 ± 0.009**	**This work**	**1994†**

Uncertainties correspond to ±1σ.
† Several locations.

Table 8
Radium and uranium activities in water samples from a number of rivers around the world

River	^{226}Ra (mBq l^{-1})	U (μg l^{-1})	Reference	Location, Date
Guadalquivir	2 - 20	1 - 3	Martínez-Aguirre & García-León, 1992	Spain, 1984-89†
Odiel		1.13 - 63.10	Martínez-Aguirre & García-León, 1991	Huelva (Spain), 1988
Guadiana		4.86 - 10.53	Vera Tomé et al. , 1988	Spain
Júcar		0.57 - 2.40	Rodríguez, 1993	Spain
Mosela, Sena, Ródano, Loira & Garona	0 - 140	0 - 11	Descamps & Foulquier, 1988	France, 1967-87
Var & Tavignano	1 - 35	0.08 - 3	Descamps & Foulquier, 1988	France, 1967-87
Sava	0.5 - 25	0.2 - 0.6	Kobal et al., 1990	Slovenia, 1975
Severn		0.3 - 2.8	Hesketh, 1982	United Kingdom, 1980
World mean	3	0.3 - 0.6	Scott, 1982	Several countries
Ebro	**28.2 ± 0.8**	**1.3 ± 0.2**	**This work**	**Spain, 1994†**

Uncertainties correspond to ±1σ.
† Several locations.

Table 9
^{3}H, ^{90}Sr and ^{137}Cs activities in water from a number of rivers around the world

River	^{3}H (Bq l^{-1})	^{90}Sr (mBq l^{-1})	^{137}Cs (mBq l^{-1})	Reference	Location, date
Ebro	0.20 - 17.04			CSN, 1993	Spain, 1992†
Tajo	1.53 - 33.86			CSN, 1993	Spain, 1992†
Guadiana	1.20			CSN, 1993	Balbuena (Spain), 1992
Duero	3.55			CSN, 1993	Soria (Spain), 1992
Tajo	1.1 - 20	0.8 -3.2	1.1 - 9.0	Carreiro et al., 1991; Carreiro & Sequeira, 1994	Portugal, 1986-93
Guadiana	0.3 - 2.4	0.6 -1.6	0.5 - 1.4	Carreiro & Sequeira, 1994	Portugal, 1989-93
Var			0.7 - 2.7	Fukai et al., 1981	France, 1977
Ródano			1.7 - 9.0	Fukai *et al*., 1981	France, 1977
Ródano	10.0 - 38.3	10 - 50		CBRMC, 1992	France,1977-81
Severn	9 - 12	6 - 12		Hesketh, 1982	United Kingdom, 1980
Ebro	**< 2.6 - 6.7**	**6.6 ± 0.3**	**< 0.64**	**This work**	**1994†**

Uncertainties correspond to ±1σ.
† Several locations.

Figure captions

Fig. 1. Minerals, rocks and geological terrains of the Ebro river basin.

Fig. 2. Industry, agricultural areas and population of the Ebro river basin.

Fig. 3. Map of the Ebro river basin showing the sampling locations (November 1994). Numbers of the sampling locations in the map correspond with YY of the code samples (EB94XXYY) shown in Table 1.

Fig. 4. Distribution of gross alpha activity in the Ebro river basin (November 1994). The gross alpha activity in the main course is shown in the left bottom corner.

Fig. 5. Distribution of the gross beta activity in the Ebro river basin (November 1994). The gross beta activity in the main course is shown in the left bottom corner.

Fig. 6. Distribution of the radium activity in the Ebro river basin (November 1994). The radium activity in the main course is shown in the left bottom corner.

Fig. 7. Distribution of the uranium mass concentration in the Ebro river basin (November 1994). The uranium mass concentration in the main course is shown in the left bottom corner.

Fig. 8. Distribution of the potassium mass concentration in the Ebro river basin (November 1994). The potassium mass concentration in the main course is shown in the left bottom corner.

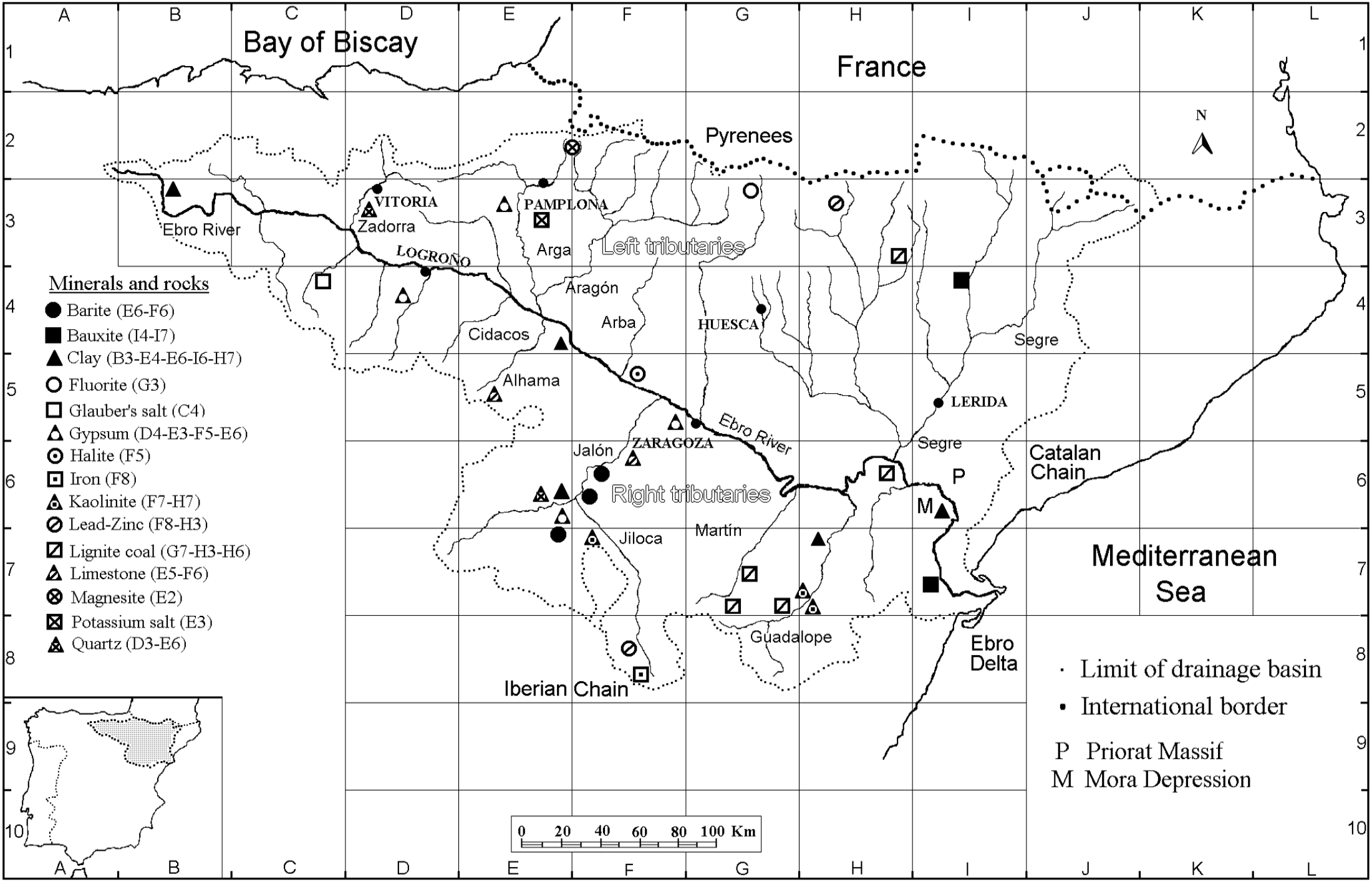

Fig. 1. Minerals, rocks and geological terrains of the Ebro river basin.

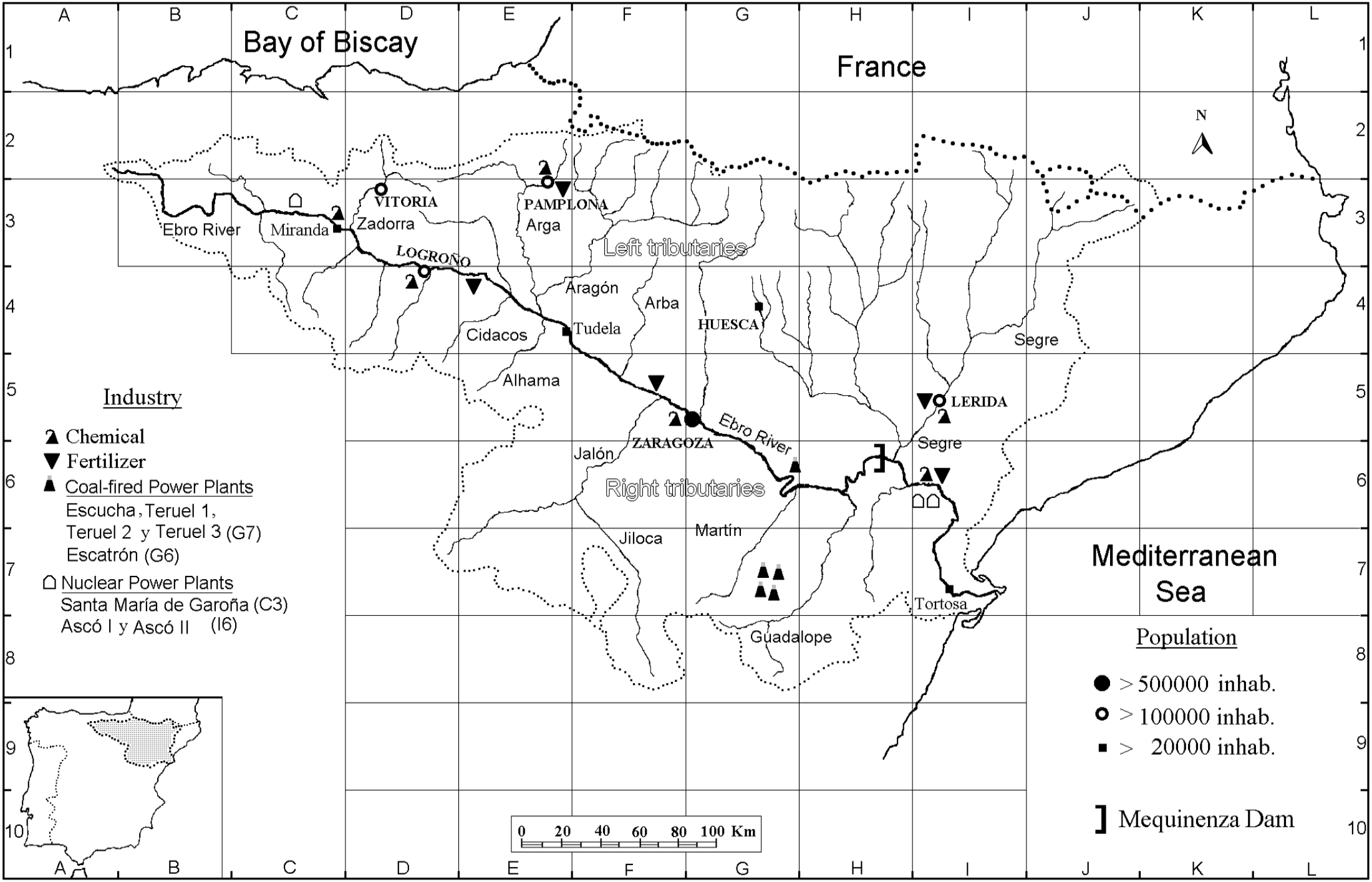

Fig. 2. Industry, agricultural areas and population of the Ebro river basin.

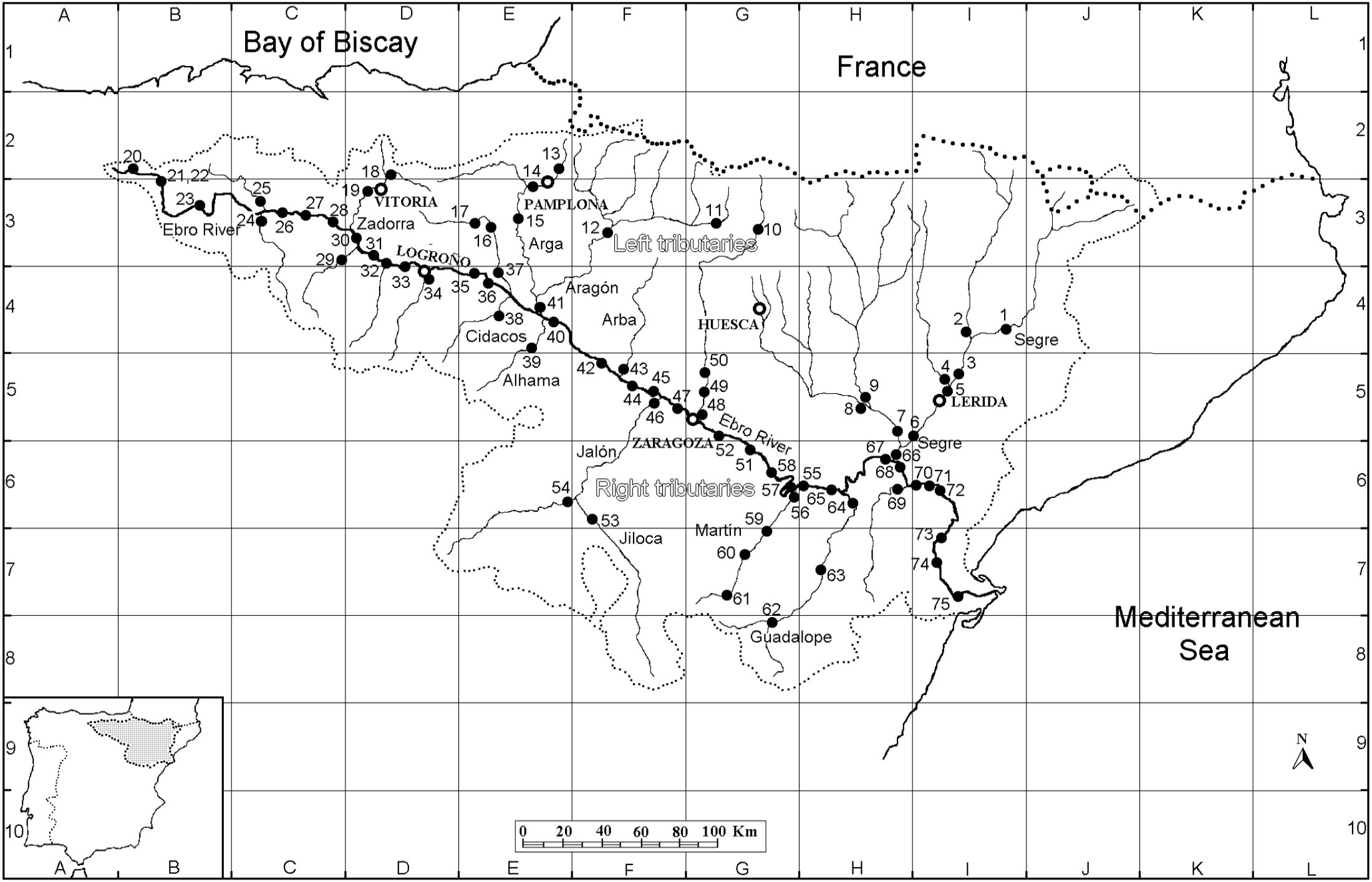

Fig. 3. Map of the Ebro river basin showing the sampling locations (November 1994). Numbers of the sampling locations in the map correspond with YY of the code samples (EB94XXYY) shown in Table 1.

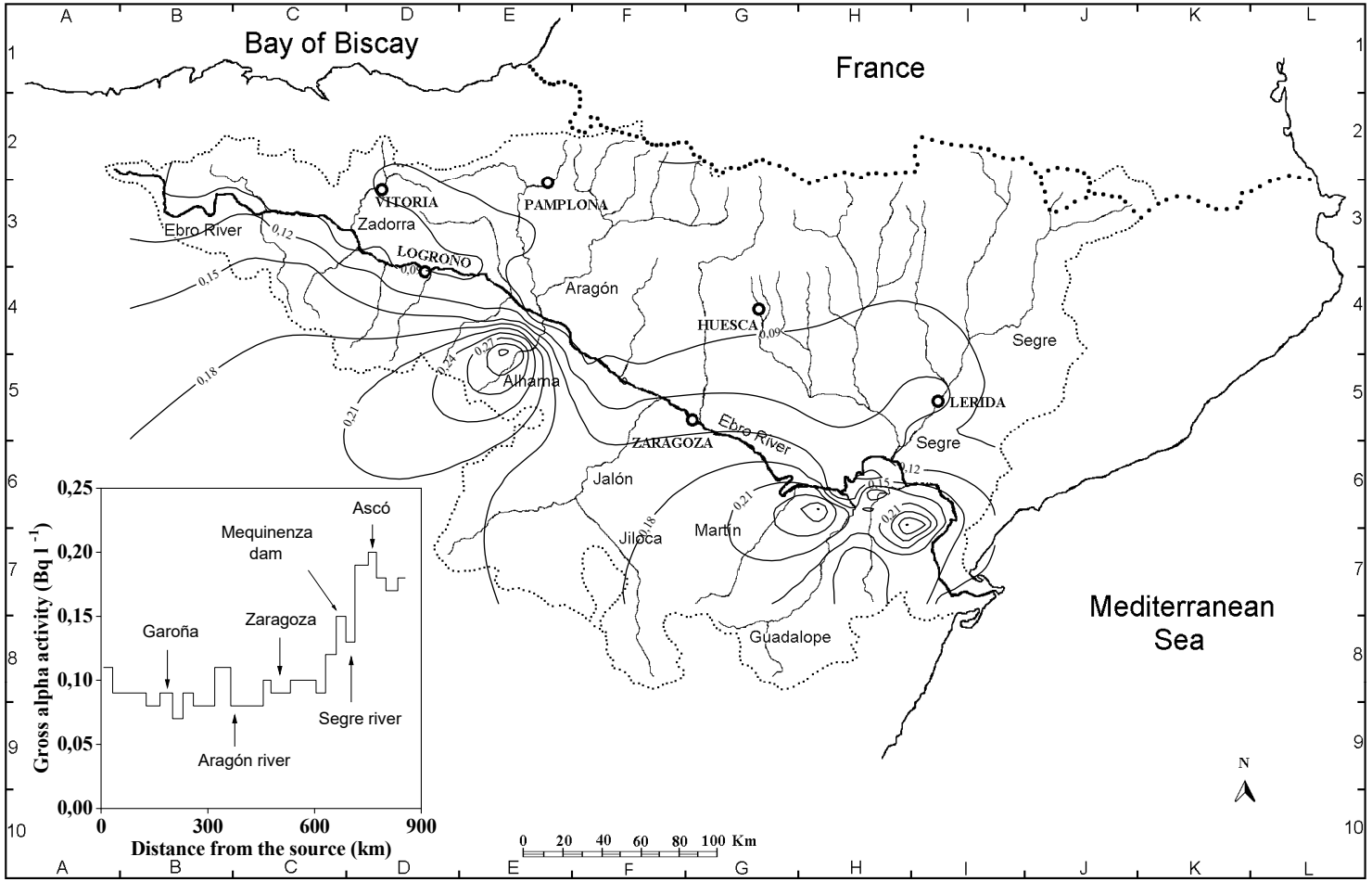

Fig. 4. Distribution of gross alpha activity in the Ebro river basin (November 1994). The gross alpha activity in the main course is shown in the left bottom corner.

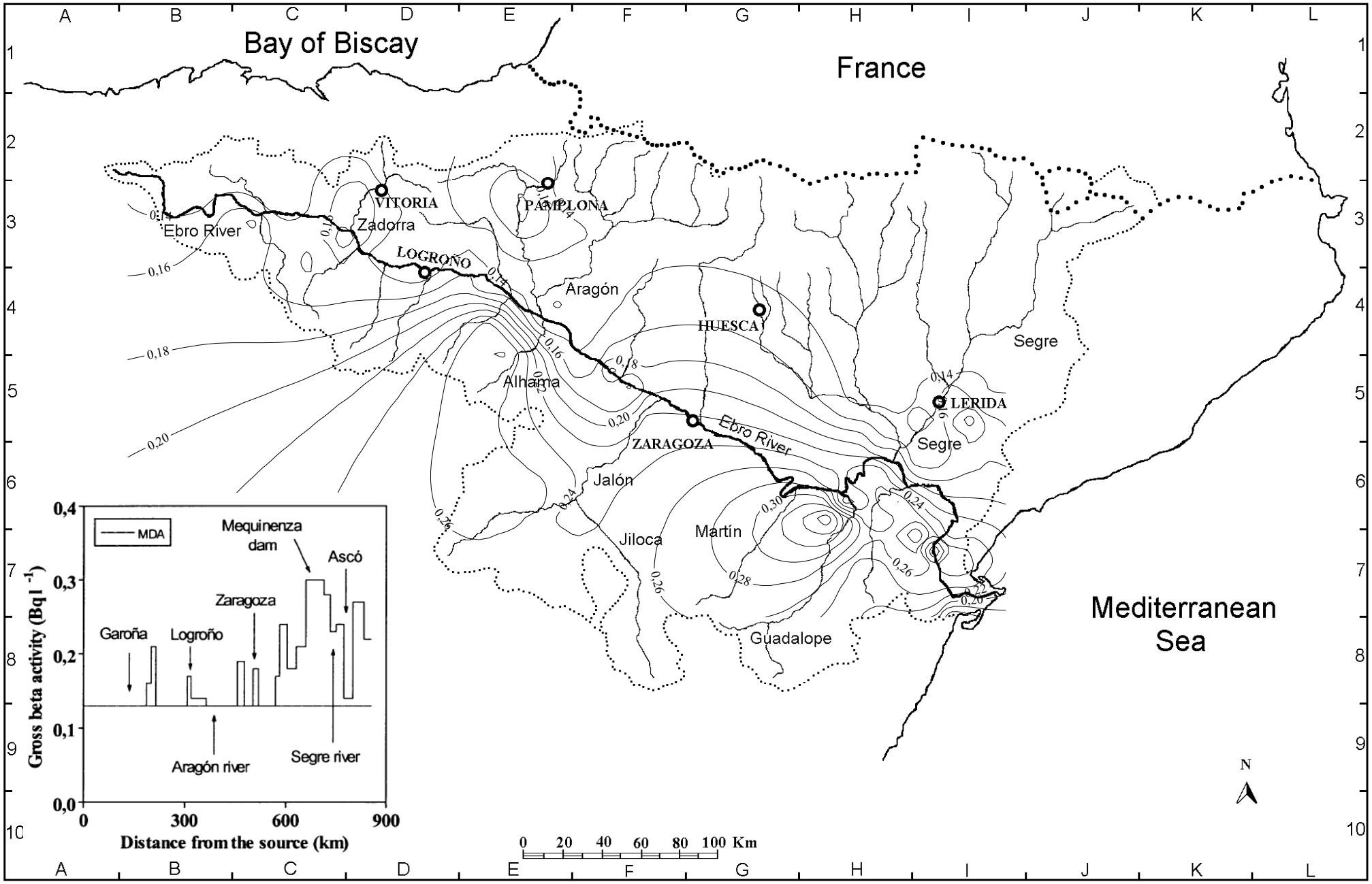

Fig. 5. Distribution of the gross beta activity in the Ebro river basin (November 1994). The gross beta activity in the main course is shown in the left bottom corner.

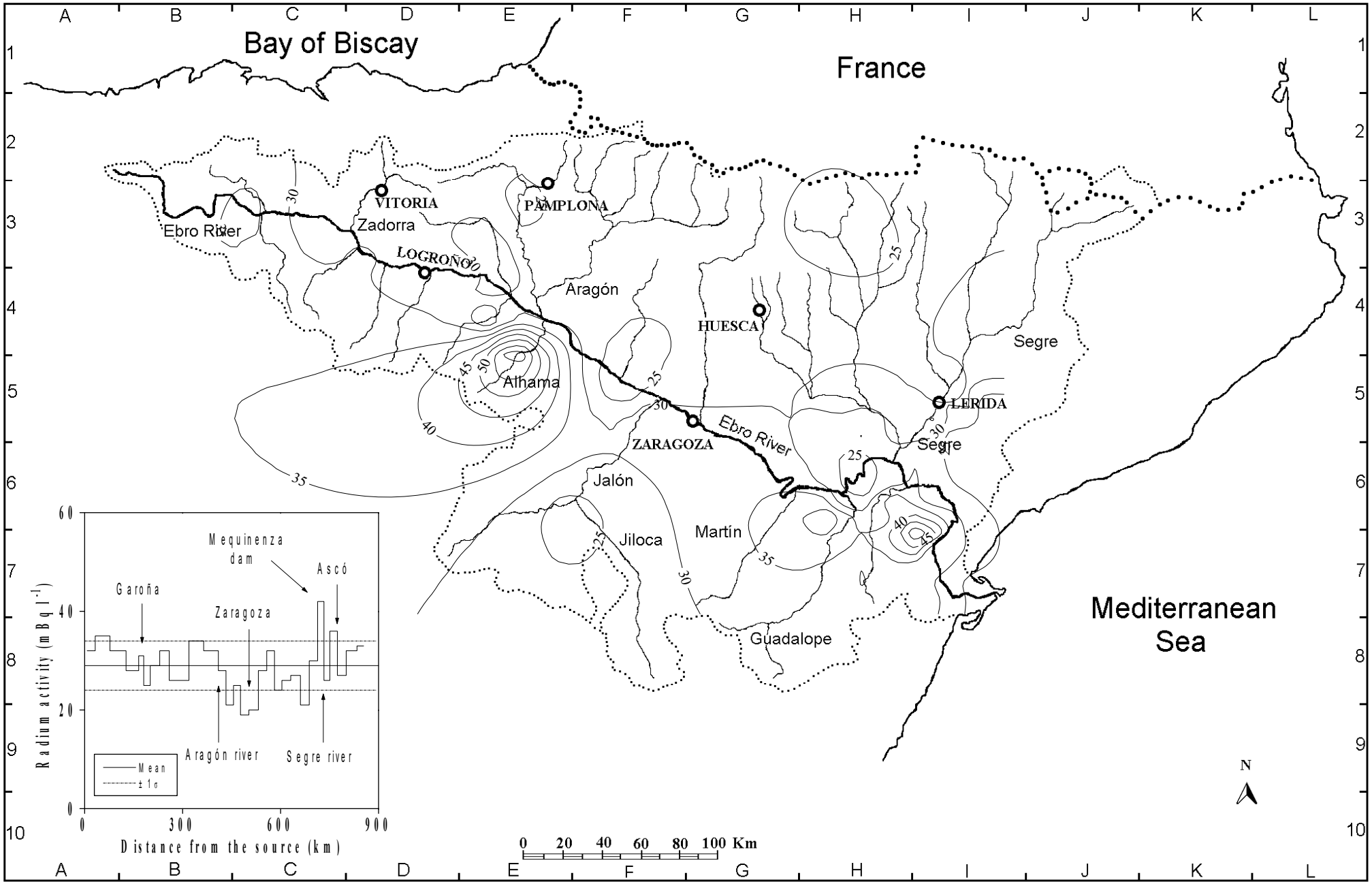

Fig. 6. Distribution of the radium activity in the Ebro river basin (November 1994). The radium activity in the main course is shown in the left bottom corner.

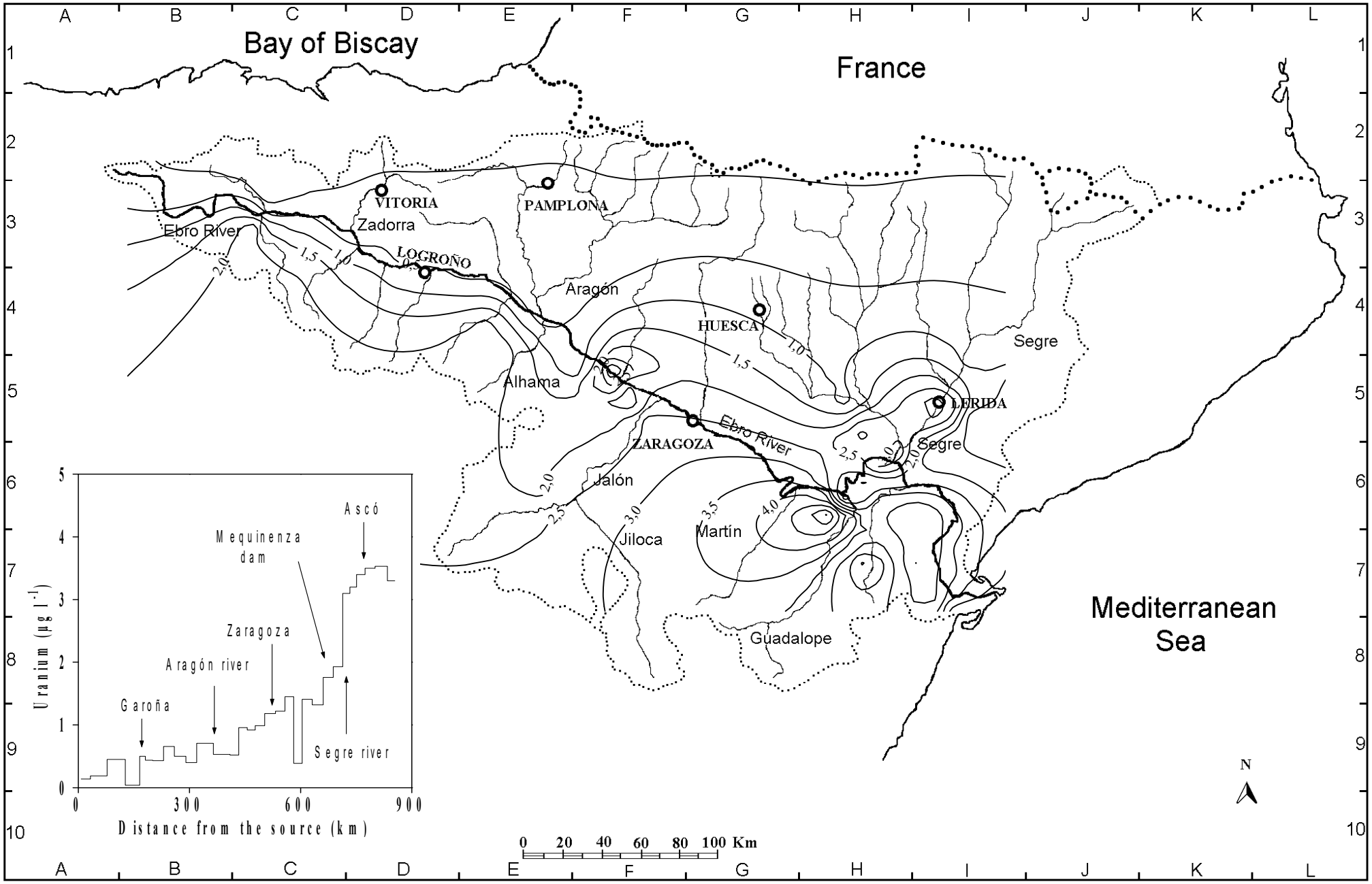

Fig. 7. Distribution of the uranium mass concentration in the Ebro river basin (November 1994). The uranium mass concentration in the main course is shown in the left bottom corner.

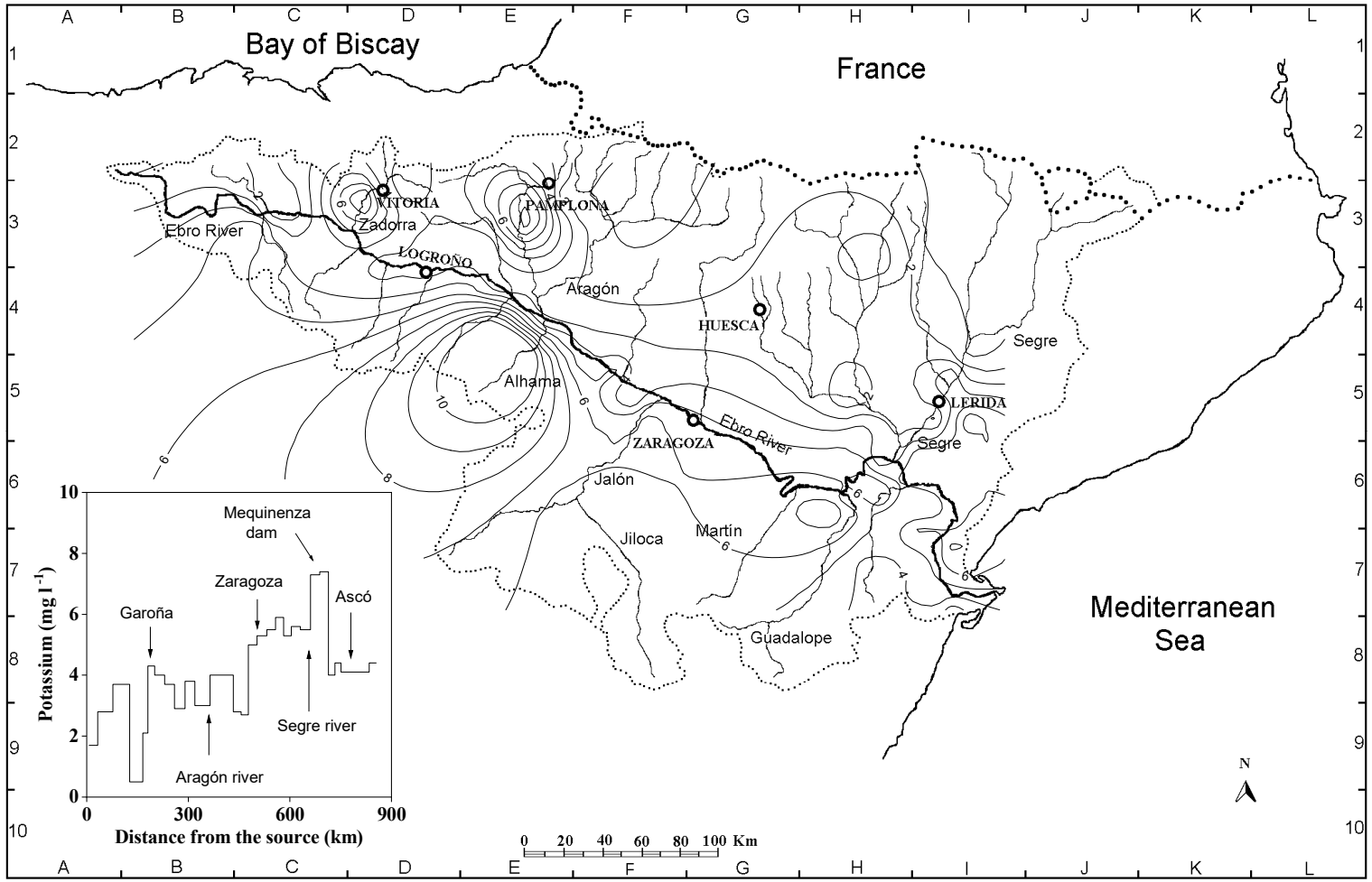

Fig. 8. Distribution of the potassium mass concentration in the Ebro river basin (November 1994). The potassium mass concentration in the main course is shown in the left bottom corner.